OPEN ACCESS Freely available online

PLoS GENETICS

Drosophila Lipophorin Receptors Mediate the Uptake of Neutral Lipids in Oocytes and Imaginal Disc Cells by an Endocytosis-Independent Mechanism

Esmeralda Parra-Peralbo, Joaquim Culi*

Centro Andaluz de Biología del Desarrollo (CSIC-UPO), Universidad Pablo de Olavide, Sevilla, Spain

Abstract

Lipids are constantly shuttled through the body to redistribute energy and metabolites between sites of absorption, storage, and catabolism in a complex homeostatic equilibrium. In *Drosophila*, lipids are transported through the hemolymph in the form of lipoprotein particles, known as lipophorins. The mechanisms by which cells interact with circulating lipophorins and acquire their lipidic cargo are poorly understood. We have found that *lipophorin receptor 1* and *2* (*lpr1* and *lpr2*), two partially redundant genes belonging to the Low Density Lipoprotein Receptor (LDLR) family, are essential for the efficient uptake and accumulation of neutral lipids by oocytes and cells of the imaginal discs. Females lacking the *lpr2* gene lay eggs with low lipid content and have reduced fertility, revealing a central role for *lpr2* in mediating *Drosophila* vitellogenesis. *lpr1* and *lpr2* are transcribed into multiple isoforms. Interestingly, only a subset of these isoforms containing a particular LDLR type A module mediate neutral lipid uptake. Expression of these isoforms induces the extracellular stabilization of lipophorins. Furthermore, our data indicate that endocytosis of the lipophorin receptors is not required to mediate the uptake of neutral lipids. These findings suggest a model where lipophorin receptors promote the extracellular lipolysis of lipophorins. This model is reminiscent of the lipolytic processing of triglyceride-rich lipoproteins that occurs at the mammalian capillary endothelium, suggesting an ancient role for LDLR–like proteins in this process.

Citation: Parra-Peralbo E, Culi J (2011) *Drosophila* Lipophorin Receptors Mediate the Uptake of Neutral Lipids in Oocytes and Imaginal Disc Cells by an Endocytosis-Independent Mechanism. PLoS Genet 7(2): e1001297. doi:10.1371/journal.pgen.1001297

Editor: Kaveh Ashrafi, University of California San Francisco, United States of America

Received August 13, 2010; **Accepted** January 7, 2011; **Published** February 10, 2011

Funding: This work was funded by grants from the European Commission (MIRG-CT-2005-021567) and the Spanish Ministerio de Ciencia e Innovación (BFU2005-01885 and BFU2008-01044) to JC and by the American Heart Association to RS Mann. Centro Andaluz de Biología del Desarrollo is institutionally supported by CSIC, Universidad Pablo de Olavide, and Junta de Andalucía. The funders had no role in study design, data collection and analysis, decision to publish, or preparation of the manuscript.

Competing Interests: The authors have declared that no competing interests exist.

* E-mail: jculesp@upo.es

Introduction

Organisms need to tightly regulate the balance between energy intake, usage and storage. Imbalances in these processes are at the heart of several major human health problems such as obesity, cardiovascular disease and diabetes [1]. In recent years, the use of *Drosophila* and other genetically tractable model organisms has provided novel approaches and insights into the study of the mechanisms controlling energy balance. In particular, genetic screens have shown their potential for the identification of novel genes and regulatory mechanisms involved in the maintenance of lipid homeostasis. Importantly, despite the evolutionary distance separating humans from flies, many of the central pathways controlling metabolism are conserved (for reviews, see [2–6]). Despite these advances, several basic aspects of *Drosophila* lipid metabolism are still unknown. Here we focus on the mechanisms controlling the cellular uptake of neutral lipids.

Most metazoans accumulate triacylglycerol (TAG), a strongly hydrophobic molecule with a high energy content, as the main substrate for energy storage. Large amounts of TAG are stored in fat body cells, the *Drosophila* equivalent of adipocytes, but most other cell types also accumulate limited amounts of it as intracellular lipid droplets. Because of their hydrophobicity, the extracellular transport of lipids requires dedicated mechanisms to increase their solubility in extracellular fluids. In mammals, lipids are packed into several types of lipoprotein particles which contain a hydrophobic core of neutral lipids (mostly TAG and esterified cholesterol) surrounded by a monolayer of phospholipids. In addition, apolipoproteins stabilize and regulate these particles [7]. Similar lipoproteins, named lipophorins, are also found in insects [8,9]. They share the same basic structure and play similar functions as mammalian lipoproteins. In *Drosophila*, apolipophorins are exclusively synthesized in the fat body [10,11], where they are partially lipidated and released into the hemolymph. It has been suggested that lipophorins act as a reusable shuttle in lipid transport. Lipids, primarily diacylglycerol (DAG), derived from the digestion of food in the gut or from the mobilization of lipids in the fat body, are loaded onto pre-formed, circulating lipophorins, then transported through the body via the hemolymph and unloaded upon reaching peripheral tissues for use as a source of energy and phospholipids. During this cycling process, negligible degradation of apolipophorin occurs [8,12].

In mammals, the Low Density Lipoprotein Receptor (LDLR) and other related proteins mediate endocytosis and the clearance of lipoproteins from plasma [13]. Similar proteins belonging to the LDLR family, known as lipophorin receptors, were subsequently identified in insects. They can bind to lipophorins and mediate their endocytosis both in cell culture systems and in vivo [14–16]. Because of these properties, it has been suggested that lipophorin receptors may play an important role in insect lipid metabolism [17].

Author Summary

Understanding the complex mechanisms that regulate the storage of caloric surpluses in the form of fat is critical in view of the public health problems caused by the continuous rise of obesity and diabetes. Important advances in the field have been obtained from studies using simple animal models like worms or flies. Here we focus on the molecular mechanisms involved in how cells capture neutral lipids from the extracellular milieu, using the fruit fly *Drosophila melanogaster* as a model organism. Lipids are transported through the blood or the insect hemolymph as small particles known as lipoproteins. We show that two *Drosophila* proteins related to the mammalian Low Density Lipoprotein Receptor, Lipophorin Receptor 1 and 2, are essential for the cellular acquisition of neutral lipids from extracellular lipoproteins. We have found that the endocytic uptake of the lipoprotein particles was not required for this process. Instead, we propose that lipophorin receptors favor the extracellular hydrolysis of lipids contained in lipoproteins, followed by uptake of the released free fatty acids. This process is similar to the extracellular processing of lipoproteins that takes place in the capillaries of mammals, suggesting an ancient role for LDLR–related proteins in the extracellular processing of lipoproteins.

Here, we examine the function of *Drosophila* lipophorin receptors in the uptake of neutral lipids. We show that this organism has two lipophorin receptor genes, the *lipophorin receptor 1 (lpr1)* and *lpr2*, which are translated into multiple, functionally diverse isoforms. *lpr1* and *lpr2* are required for neutral lipid uptake in imaginal disc cells and oocytes. Our results suggest a model where *lpr1* and *lpr2* promote the extracellular hydrolysis of neutral lipids contained in lipoprotein particles.

Results

Genomic organization and alternative splicing of *Drosophila* lipophorin receptor genes

A defining characteristic of the LDLR family of transmembrane receptors is the presence of an ectodomain containing specific combinations of three types of protein modules: LDL receptor type A modules (LA), also called complement-type repeats, EGF modules and YWTD β-propellers [18]. This structural definition was used to identify LDLR family members in the *Drosophila* genome. Of the seven genes identified (Figure S1), two are arranged in tandem and show a high degree of homology to insect lipophorin receptors. On this basis, we named then *lipophorin receptor 1* (*lpr1*) and *lpr2* (Figure 1A). The analysis of cDNA clones generated during large scale transcriptomic studies [19] suggested the existance of multiple isoforms for each gene. To further characterize the range of isoforms derived from *lpr1* and *lpr2*, we obtained additional cDNAs from whole adult fly RNA, as well as from RNA purified from specific tissues. These cDNAs were genotyped by PCR and sequenced, leading to the identification of a total of 6 isoforms for *lpr1* and 5 for *lpr2* (Figure 1B). The different isoforms result from alternative splicing and from the use of two alternative promoters for each gene, that we named proximal and distal promoters, referring to their chromosomal position with respect to the centromere. The number and organization of exons are remarkably similar between the two genes, with *lrp1* and *lpr2* exons in equivalent positions coding for equivalent protein domains. Isoforms differ in three main characteristics: (1) the number and identity of LA modules; (2) the presence of an extended putative O-glycosylation region rich in serine and threonine next to the transmembrane domain and (3) the presence of an N-terminal domain with no homology to other proteins (non-conserved N-terminal domain, NCN) (Figure 1B). It is noteworthy that isoforms transcribed from the distal promoters are predicted, using PrediSi software [20], to have unusually long putative signal peptides: 68 and 88 amino acids for *lpr1* and *lpr2*, respectively. Isoforms transcribed from the proximal promoters are predicted to have more typical signal peptides of 20 (*lpr1*) and 24 (*lpr2*) amino acids.

lpr1 and *lpr2* are required for the accumulation of lipid droplets in oocytes and imaginal disc cells

To examine the role of the lipophorin receptors in lipid metabolism, we first generated three small deletions in the *lpr1-lpr2* genomic region (Figure 1A). *Df(3R)lpr1* completely deletes *lpr1*; *Df(3R)lpr2* deletes exons 1 to 8 of *lpr2*, including the promoters and translation initiation codons, while *Df(3R)lpr1/2* affects both genes. The breakpoints for each deficiency were confirmed by PCR analysis. Even though several *lpr2* exons are still present in *Df(3R)lpr2* and *Df(3R)lpr1/2* chromosomes, we did not detect Lpr2 protein expression in either deficiency using an antibody which recognizes Lpr2 intracellular domain, which is common to all Lpr2 isoforms (Figure S2C–S2F and not shown). This data strongly suggests that *Df(3R)lpr2* is a null allele for *lpr2* and *Df(3R)lpr1/2* is a null allele for both *lpr1* and *lpr2*. Flies with mutations in individual lipophorin receptor genes as well as the double mutant *Df(3R)lpr1/2* were homozygous viable and displayed fertility phenotypes: *Df(3R)lpr1* females laid eggs which hatched at rates similar to wild-type females (85.5% hatching rate for *Df(3R)lpr1* compared to 87.5% for the wild-type stock Oregon R, n = 200). *Df(3R)lpr2* females laid eggs but most of them failed to hatch (0.5% hatching rate; n = 200). *Df(3R)lpr1/2* females were completely sterile, where the few eggs laid by young flies failed to hatch. These results indicate that *lpr2*, and to a lesser extent *lpr1*, are required for normal oogenesis. The *Drosophila* ovarian follicle is composed of a 16-cell germ-line cyst with one oocyte and 15 nurse cells, which is surrounded by somatic follicle cells. During vitellogenesis, the oocyte and nurse cells increase in volume and accumulate large amounts of yolk proteins and neutral lipids (Figure 2F–2I) that are captured from the surrounding hemolymph [21]. The Yolkless (Yl) receptor mediates the endocytic uptake of yolk proteins [22,23]. However, no receptor involved in lipid uptake has been reported. To analyze whether *lpr1* or *lpr2* mediate lipid uptake during vitellogenesis, we first examined the lipid content of ovaries from wild-type and *Df(3R)lpr2* females with the lipophilic nile red dye. Accumulation of neutral lipids was first visible in stage 9 wild-type egg chambers and reached a maximum by the end of vitellogenesis at stage 11 (Figure 2F–2I). A marked decrease in lipid droplets was observed in *Df(3R)lpr2* egg chambers (Figure 2J, compare to Figure 2G. Figure S3A) or when this deficiency was combined with the double mutant *Df(3R)lpr1/2* (not shown). Most of the embryos originating from *Df(3R)lpr2* mutant oocytes could not complete embryogenesis and died at various stages of development, showing generalized apoptosis and pleiotropic phenotypes such as muscle detachment and nervous system malformations (not shown). A small number of *Df(3R)lpr2* egg chambers exhibited higher lipid levels (Figure S3A). It seems likely that the few embryos that successfully hatched from *Df(3R)lpr2* females (0.5%) were derived from these egg chambers.

We used a Lpr2-specific antibody to examine the distribution of Lpr2 in wild-type egg chambers, detecting Lpr2 protein at the membranes of nurse cells and oocytes in vitellogenic egg chambers (Figure 2C–2E). This expression was low at the beginning of

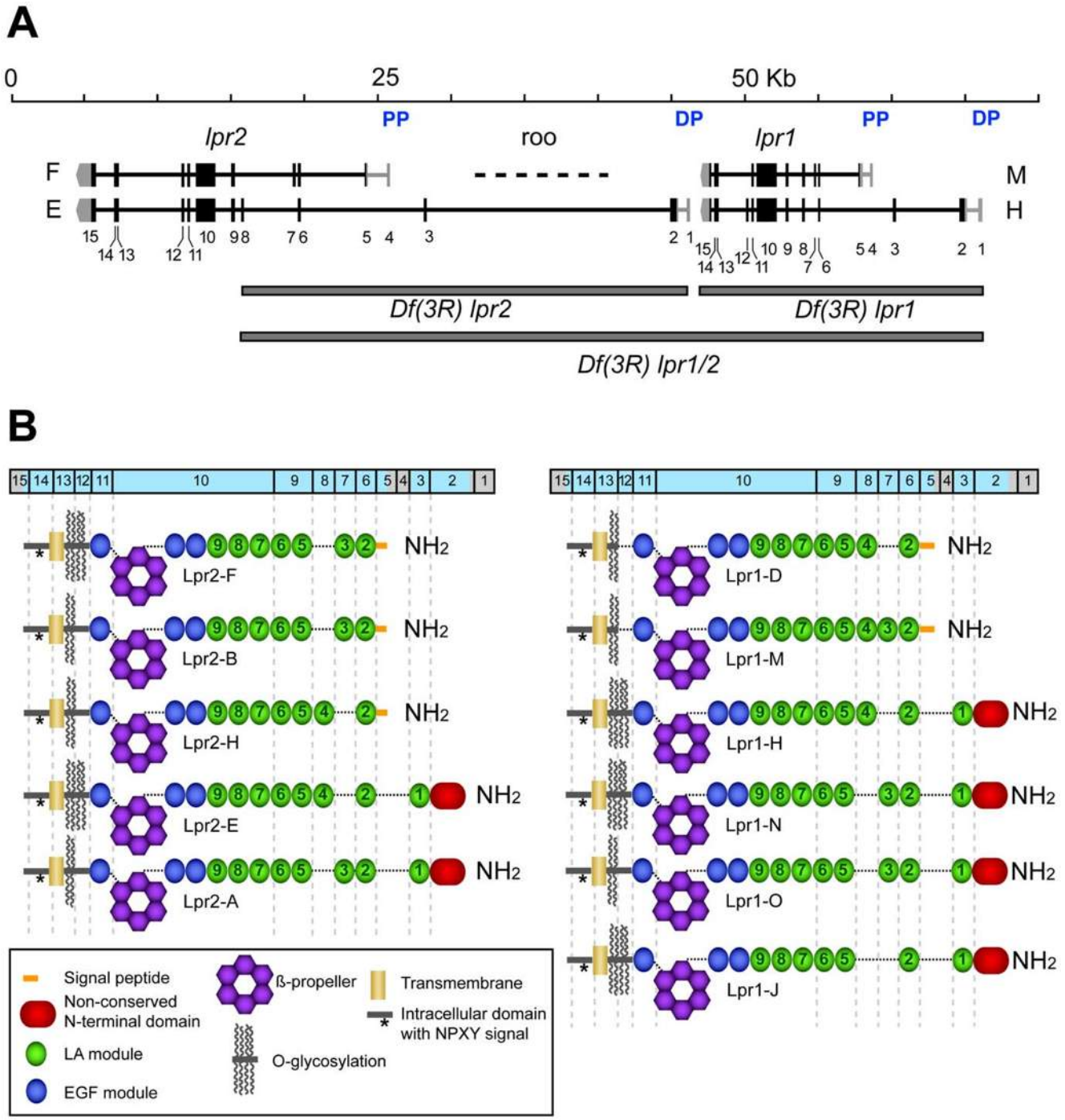

Figure 1. Genomic organization of *lpr1* and *lpr2* genes. (A) *lpr1* and *lpr2* are transcribed as multiple isoforms. Each gene has two promoters, a distal promoter (DP) and a proximal promoter (PP). Only one isoform transcribed from each promoter is displayed in the figure. The complete list of isoforms is detailed in panel B. Exons are labeled from 1 to 15. We generated three deficiencies *Df(3R)lpr1*, *Df(3R)lpr2* and *Df(3R)lpr1/2*, which are indicated as grey rectangles. A natural roo transposon is present in the second *lpr2* intron. (B) Modular structure of Lpr1 and Lpr2 isoforms, showing the correspondence between protein domains and exons (blue box on top). The existence of all depicted isoforms is supported by the isolation of corresponding cDNAs. The UTR regions are marked in grey.
doi:10.1371/journal.pgen.1001297.g001

vitellogenesis (stage 8, Figure 2C asterisk) and increased as the egg chamber matured, being maximal at stage 11 (Figure 2E). In situ hybridization detected a similar expression pattern for *lpr2* transcripts (Figure 2B). Together, these results demonstrate that Lpr2 is the major receptor involved in the uptake of neutral lipids by nurse cells and oocytes. In contrast, our results indicate that *lpr1* is not essential for this process since egg chambers from *Df(3R)lpr1* females had normal amounts of neutral lipids (Figure 2L, Figure S3A). However, *lpr1* appears to play some role in oogenesis since *Df(3R)lpr1/2* females, which lack both receptors, exhibited stronger and qualitatively distinct phenotypes compared to *Df(3R)lpr2* mutants. Ovaries from *Df(3R)lpr1/2* females were

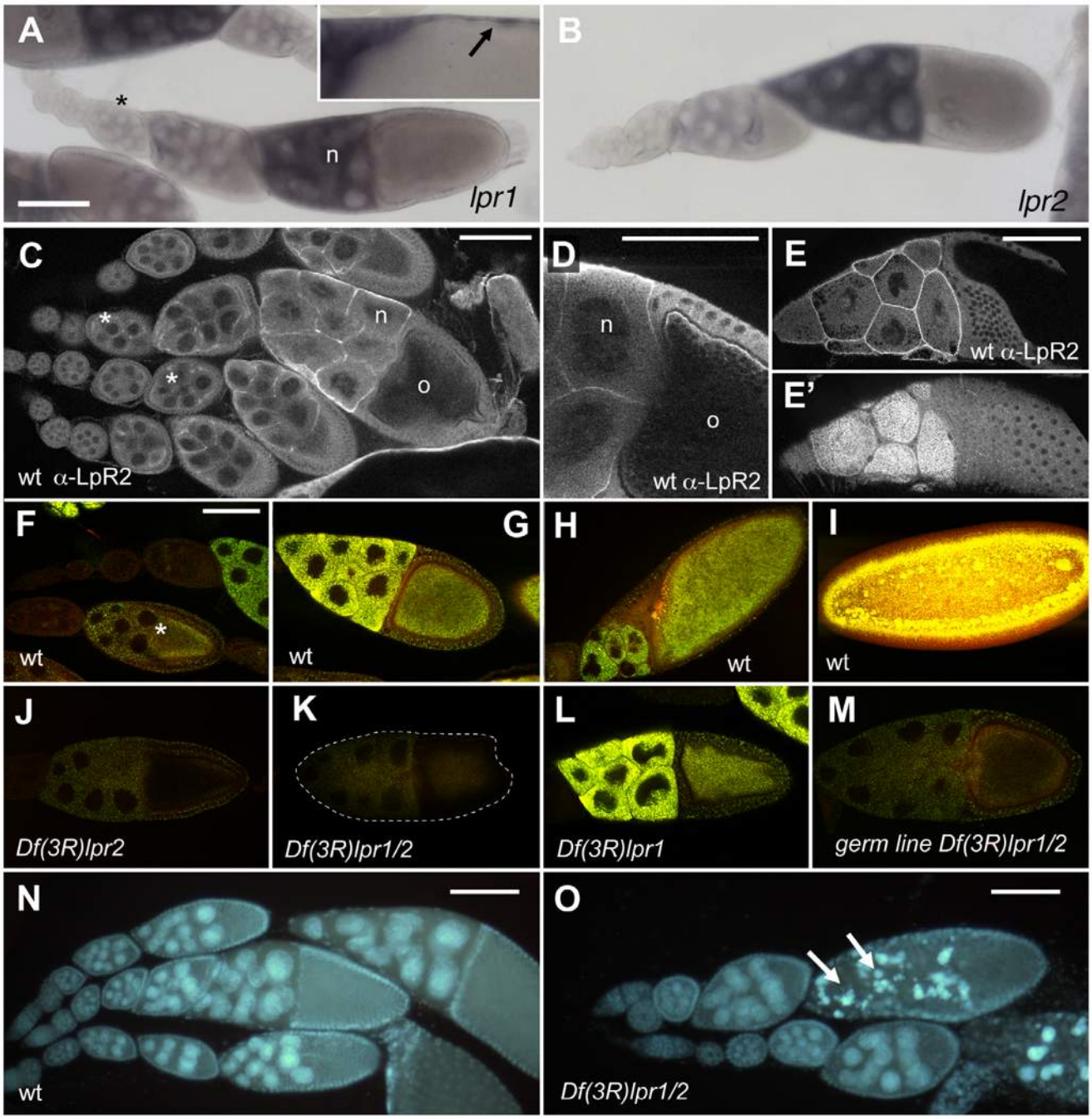

Figure 2. Lpr2 is required for the uptake of neutral lipids during *Drosophila* vitellogenesis. (A–B) *lpr1* (A) and *lpr2* (B) expression in wild-type ovarioles detected by in situ hybridization. Transcripts of both genes were first visible in the nurse cells (n) of stage 8 egg chambers (asterisk) and their levels increased thereafter. *lrp1* transcripts were also detected in the follicle cells of mature egg chambers (A, arrow in inset). (C–E) Immunostaining showing Lpr2 protein localization during oogenesis. Lpr2 is first detected at low levels in stage 8 egg chambers, coinciding with the start of vitellogenesis (asterisks in C). (D) Magnification of a stage 10 egg chamber showing expression at the nurse cells (n) and oocyte (o) membranes. Maximal expression was detected at stage 11 egg chambers (E and E′, two focal planes). (F–M) Nile red staining of egg chambers (F–H and J–M) and one blastoderm stage embryos (I) to reveal lipid droplets (yellow, nile red dye fluorescence was captured in the green and red channels). (F–I) Wild-type (wt) genotype. Neutral lipids start to accumulate at vitellogenic stages and reach a maximum in blastoderm embryos. Note that near the end of vitellogenesis, nurse cells degenerate and dump their content into the oocyte. (F) stage 9 (asterisk), (G) stage 10 and (H) stage 11 egg chambers. (J–M) stage 10 egg chambers of the indicated genotypes. Accumulation of neutral lipids is reduced in *Df(3R)lpr2* (J), *Df(3R)lpr1/2* (K, egg chamber outlined) and *Df(3R)lpr1/2* germ-line clones (M) and is normal in *Df(3R)lpr1* egg chambers (L). The *Df(3R)lpr1/2* egg chamber shown in (K) was dissected from young females in which a few egg chambers in each ovary escaped degeneration at mid oogenesis. (N, O) Egg chambers of wild-type (N) and *Df(3R)lpr1/2* (O) ovaries stained with DAPI to reveal the nuclei. Several stage 10 egg chambers display nuclear fragmentation in *Df(3R)lpr1/2* females (arrows in O). Scale bars: 100 μm. (F–M) shown at the same magnification.
doi:10.1371/journal.pgen.1001297.g002

severely reduced in size and contained abundant cellular debris. DAPI staining revealed condensation and fragmentation of the nurse cell nuclei at stages 9–10, indicating cell degeneration (Figure 2O, compare to Figure 2N. Figure S3B), a phenotype not observed in *Df(3R)lpr2* females, explaining the egg laying phenotype described for these mutants earlier. Starvation and other adverse stimuli are known to activate an oogenesis checkpoint that results in the apoptosis of egg chambers at mid-oogenesis [24]. Thus, the degeneration of *Df(3R)lpr1/2* ovaries probably results from activation of this checkpoint. As expected, the few non-degenerating stage 10 egg chambers that can be found in young *Df(3R)lpr1/2* females had extremely low lipid content (Figure 2K). These results indicate that *lpr1* has a partially redundant function during oogenesis, which was only revealed in the absence of *lpr2*. Accordingly, we detected *lpr1* expression in nurse cells and follicle cells by in situ hybridization and RT-PCR (Figure 2A, Figure 5G) but not by antibody staining (not shown), suggesting that Lrp1 protein levels might be low. Oogenesis is a complex process regulated by hormonal signals that relay information about the nutritional status of the female and other stimuli [25]. Thus, it is conceivable that mutations in *lpr1* and *lpr2* could affect oogenesis, at least in part, by altering the hormonal or nutritional status of the female. To address this point, we eliminated *lpr1* and *lpr2* exclusively in the oocyte and nurse cells by generating *Df(3R)lpr1/2* germ-line clones. The resulting females were sterile but laid abundant non-viable eggs, the egg chambers had low lipid content (Figure 2M) and no signs of degeneration were observed at mid oogenesis (not shown). Taken together, these experiments indicated that *lpr2* and to a minor extent *lpr1*, are autonomously required in the oocyte and nurse cells to mediate lipid uptake during vitellogenesis. In addition, they suggest that somatic expression of the lipophorin receptors contributes to the regulation of the mid-oogenesis checkpoint.

To examine whether *lpr1* or *lpr2* are involved in lipid uptake in other tissues, we analyzed larval imaginal discs, an epithelial tissue known to accumulate abundant intracellular lipid droplets [26]. Wild-type wing imaginal discs displayed strong neutral lipid accumulation in the wing pouch region (Figure 3A). In contrast, *Df(3R)lpr1/2* wing imaginal discs exhibited severely reduced levels of intracellular lipids droplets (Figure 3B), suggesting that lipophorin receptors might mediate neutral lipids uptake in imaginal disc cells in a similar way to the oocyte. Significantly, animals with single mutations in *lpr1* or *lpr2* did not exhibit this strong phenotype: *Df(3R)lpr1* discs were undistinguishable from wild-type discs (Figure 3C) while *Df(3R)lpr2* discs showed a mild reduction in lipid droplet content (Figure 3D), indicating that the functions of *lpr1* and *lpr2* are mostly redundant in this tissue. Consistent with a redundant function, we detected transcripts of both *lpr1* and *lpr2* in the wing pouch region by in situ hybridization (Figure 3E, 3F and [27]). High levels of Lpr2 protein were also detected in the wing pouch by immunostaining, with two stripes of lower expression along the antero-posterior and dorso-ventral compartment borders (Figure 3G, 3H).

To examine whether *Drosophila* lipophorin receptors had an impact on total lipid content, we measured total TAG content in *Df(3R)lpr1*, *Df(3R)lpr2* and *Df(3R)lpr1/2* male flies under a normal diet as well as under starvation conditions. No differences were observed between the three genotypes and the wild-type control (Figure S4A–S4F and Text S1). The fat body stores most of the fly's TAG reserves and in agreement with our previous results, we did not observe differences in the number or size of lipid droplets in the fat body of *Df(3R)lpr1/2* and control animals (Figure S4G–S4J), suggesting that TAG storage in the fat body is independent of the lipophorin receptors. Finally, since impaired neutral lipid

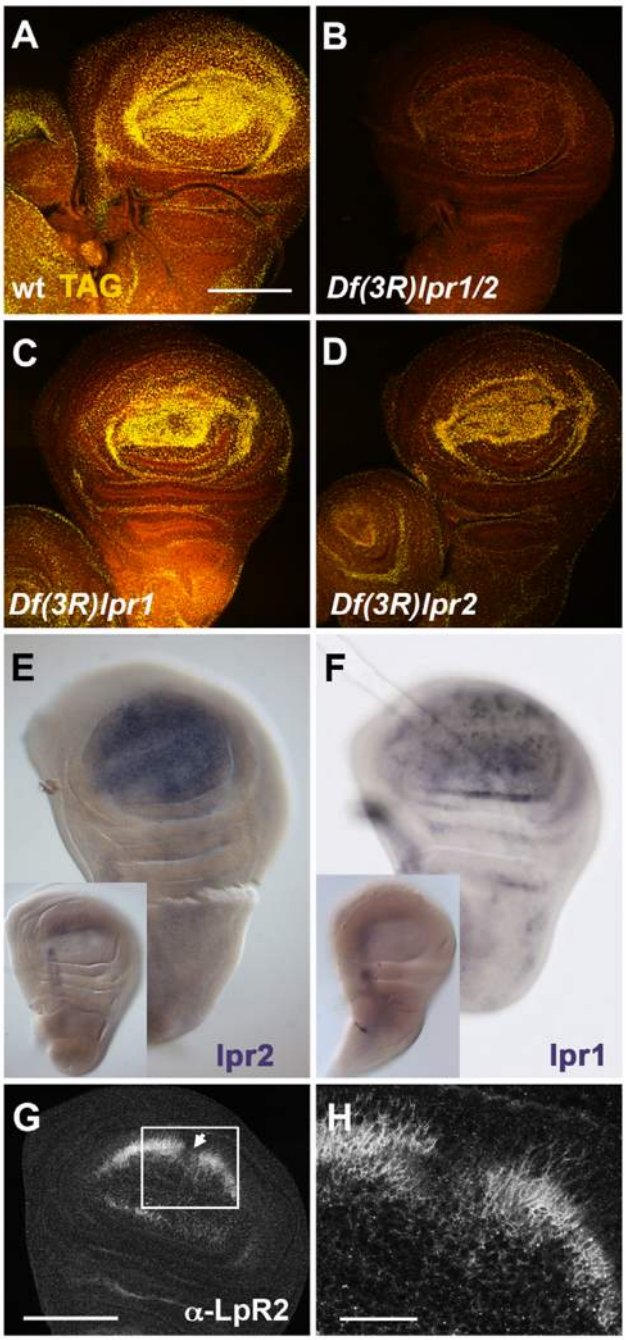

Figure 3. *lpr1* and *lpr2* are required for the uptake of neutral lipids by wing imaginal disc cells. (A–D) Wild-type (A), *Df(3R) lpr1/2* (B), *Df(3R)lpr1* (C) and *Df(3R)lpr2* (D) wing imaginal discs stained with nile red to reveal lipid droplets (yellow). In $lpr1^{-}$, $lpr2^{-}$ double mutant there is a sharp decrease in lipid accumulation (B) whereas $lpr2^{-}$ discs display a mild reduction (D). (E, F) in situ hybridization to detect *lpr2* (E) and *lpr1* (F) mRNA expression in wild-type wing imaginal discs. Both genes are mainly expressed in the wing pouch area. Insets show a *Df(3R)lpr1/2* disc (E) and a *Df(3R)lpr1* disc (F) as negative controls. (G–H) Immunostaining with α-Lpr2 antibody detected expression in the wing pouch area of wild-type imaginal discs with minimal expression near the antero-posterior (arrow) and dorso-ventral compartment boundaries. (H) Magnification of the disc shown in (G). Lpr2 accumulates at baso-lateral membranes. Scale bars: 100 μm (A, G) and 25 μm (H). (A–F) shown at the same magnification.
doi:10.1371/journal.pgen.1001297.g003

uptake by peripheral tissues could have an impact on circulating lipid levels, we measured TAG content in the hemolymph of control, *Df(3R)lpr1*, *Df(3R)lpr2* and the double mutant animals. We did not observe statistically significant differences between the four genotypes (Figure S4K and Text S1).

Only a subset of lipophorin receptor isoforms mediates the uptake of neutral lipids

lpr1 and *lpr2* are transcribed as multiple isoforms (Figure 1B), raising the issue of whether they share similar properties regarding lipid uptake. To answer this question, we first compared the isoforms transcribed from the corresponding distal versus proximal promoters. We generated two HA-tagged transgenes that allowed controlled expression of Lpr2F isoform (*UAS-lpr2F*) and Lpr2E isoform (*UAS-lpr2E*) and examined their ability to rescue lipid uptake in *Df(3R)lpr1/2* animals. Expression of *UAS-lpr2E* in the posterior compartment of the wing imaginal disc driven by *en-gal4* completely rescued lipid accumulation in that compartment (Figure 4A). In contrast, expression of *UAS-lpr2F* did not rescue lipid uptake (Figure 4B). In a similar assay, we found that whereas Lpr1H isoform rescued lipid uptake, expression of Lpr1D did not (Figure 4C, 4D). Equivalent results were obtained when we examined the role of these isoforms during vitellogenesis. Germ-line expression of *UASp-lpr1J* or *UASp-lpr2E*, driven by *V32-gal4*, rescued oogenesis and fertility of *Df(3R)lpr1/2* females. The amount of lipid droplets accumulated in nurse cells was similar to the wild-type (Figure 5C, 5E, compare to wild-type in Figure 2G) and the number of degenerating egg chambers was dramatically reduced (Figure 5D, 5F and Figure S3B). In contrast, expression of *UASp-lpr2F* did not rescue fertility, lipid uptake nor egg chamber degeneration (Figure 5A, 5B).

The LA-1 module, present in all isoforms transcribed from the distal promoters, defines the capacity to mediate neutral lipid uptake

The surprising finding that only a subset of *lpr1* and *lpr2* isoforms tested were able to mediate lipid uptake prompted us to examine the essential protein domains required for this function. Lipid uptake-promoting isoforms Lpr1H and Lpr2E are both transcribed from the corresponding alternative distal promoters and contain a non-conserved N-terminal domain (NCN) adjacent to the LA module 1 (LA-1), encoded by exons 2 and 3 respectively. In contrast, these domains are not present in the lipid uptake-defective Lpr2F and Lpr1D isoforms (Figure 1B). Thus, a sequence critical for the uptake of neutral lipids may lie in this N-terminal region. However, given that Lpr1H and Lpr2E both contain eight LA modules whereas Lpr2F and Lpr1D have seven, it is also possible that the total number of LA modules is the key factor in defining lipid uptake function. To test the role of the NCN and LA-1, we made a chimeric protein identical to Lpr2F except for its signal peptide, which was replaced with the NCN and LA-1 domains from Lpr2E, generating *UAS-lpr2F+LA1+NCN*. Overexpression of this transgene in the posterior compartment of *Df(3R)lpr1/2* wing imaginal discs completely rescued the accumulation of lipid droplets in this compartment (Figure 4F), demonstrating that this N-terminal segment was able to confer lipid uptake activity. To analyze whether NCN, LA-1 or both domains were required, we prepared two more transgenes. In *UAS-lpr2F+LA1*, the LA-1 domain from Lpr2E was inserted in between the signal peptide and LA-2 of Lpr2F. In *UAS-lpr2F+NCN*, the lpr2F signal peptide was replaced by the lpr2E NCN domain (Figure 4G, 4H). Using our rescue assay, only *UAS-lpr2F+LA1* was able to mediate lipid uptake (Figure 4G, 4H). Thus, the NCN domain, even though present in all tested lipid uptake-promoting isoforms, was not essential for this function. These results suggested that the LA-1 module was critical for the uptake of neutral lipids. However, we still could not exclude the possibility that it is the number rather than the identity of LA modules that determines lipid uptake capacity. To analyze this possibility, we examined the Lpr1J isoform which is identical to the lipid uptake-promoting Lpr1H isoform except that it has seven LA modules due to the absence of LA-4. In our rescue assay, Lpr1J did mediate lipid uptake (Figure 4E), indicating that it is the presence of LA-1 and not the number of LA modules that defines the ability to mediate lipid uptake. Moreover, in an additional transgene we modified Lpr2F by introducing a tandem duplication of LA-2, so that the new protein (Lpr2F+LA2) had eight LA modules but still lacked LA-1. Lpr2+LA2 did not mediate lipid uptake, confirming our previous conclusion (Figure 4I). Taken together, these experiments indicate that the key property that distinguishes lipid uptake-promoting from lipid uptake-defective isoforms is the presence of the LA-1 domain. It should be noted that all isoforms containing LA-1 are transcribed from the distal promoters. Consistent with the lipid uptake phenotypes of *Df(3R)lpr1/2* mutants in wing imaginal discs and ovaries, RT-PCR experiments showed that the predominant *lpr1* and *lpr2* isoforms expressed in these tissues were transcribed from the distal promoters and thus contained the LA-1 domain (Figure 5G).

Endocytosis is not required for the uptake of neutral lipids in the oocyte or imaginal discs

During the rescue experiments described in the previous sections, we realized that expression of *UAS-lpr2E* in the posterior compartment driven by *en-gal4* not only autonomously rescued lipid uptake in that compartment but also promoted the formation of lipid droplets in a one to two cells wide region of anterior tissue abutting the anterior-posterior compartment border (Figure 6B, arrow). Analysis of confocal sections spanning the thickness of the imaginal disc confirmed that cells not expressing *UAS-lpr2E* but adjacent to expressing cells, accumulated higher levels of lipid droplets than more anteriorly located cells (Figure 6A, arrow). Similar results were obtained using a different Gal4 driver line to express *UAS-lpr2E* in the dorsal wing disc compartment (Figure S5C, S5D). To analyze whether non-autonomous lipid uptake could be detected in other tissues, we returned to the egg chamber because of its particular morphology. In the *Drosophila* egg chamber, the oocyte and nurse cells are surrounded by a closely associated somatic follicular epithelium. This allowed us to examine whether expression of the lipophorin receptors in the germ-line could non-autonomously direct lipid uptake in the follicular epithelium. Follicle cells of ovaries dissected from *Df(3R)lpr1/2* females had very few lipid droplets (Figure 6C). However, after *V32-gal4*-mediated expression of *UASp-lpr2E* exclusively in the germ-line, we observed a remarkable increase in the number and size of lipid droplets in the follicular epithelium (Figure 6D). In fact, the rescue was similar to the one obtained by the expression of the lipid uptake-promoting *UAS-lpr1J* isoform directly in the follicle cells using the follicle cell driver *CY2-gal4* (Figure 6E). These results indicated that Lpr2E can non-autonomously promote neutral lipid uptake in adjacent cells.

All members of the LDLR family are known to mediate endocytosis of ligands in clathrin coated vesicles [28]. In *Drosophila*, Lpr1 and Lpr2 have been shown to endocytose lipophorins when overexpressed in imaginal discs [11,27]. Thus, a possible hypothesis for lipophorin receptor-mediated lipid uptake is that the receptors induce the endocytosis of lipophorin particles resulting in the catabolic hydrolysis of lipids in lysosomes.

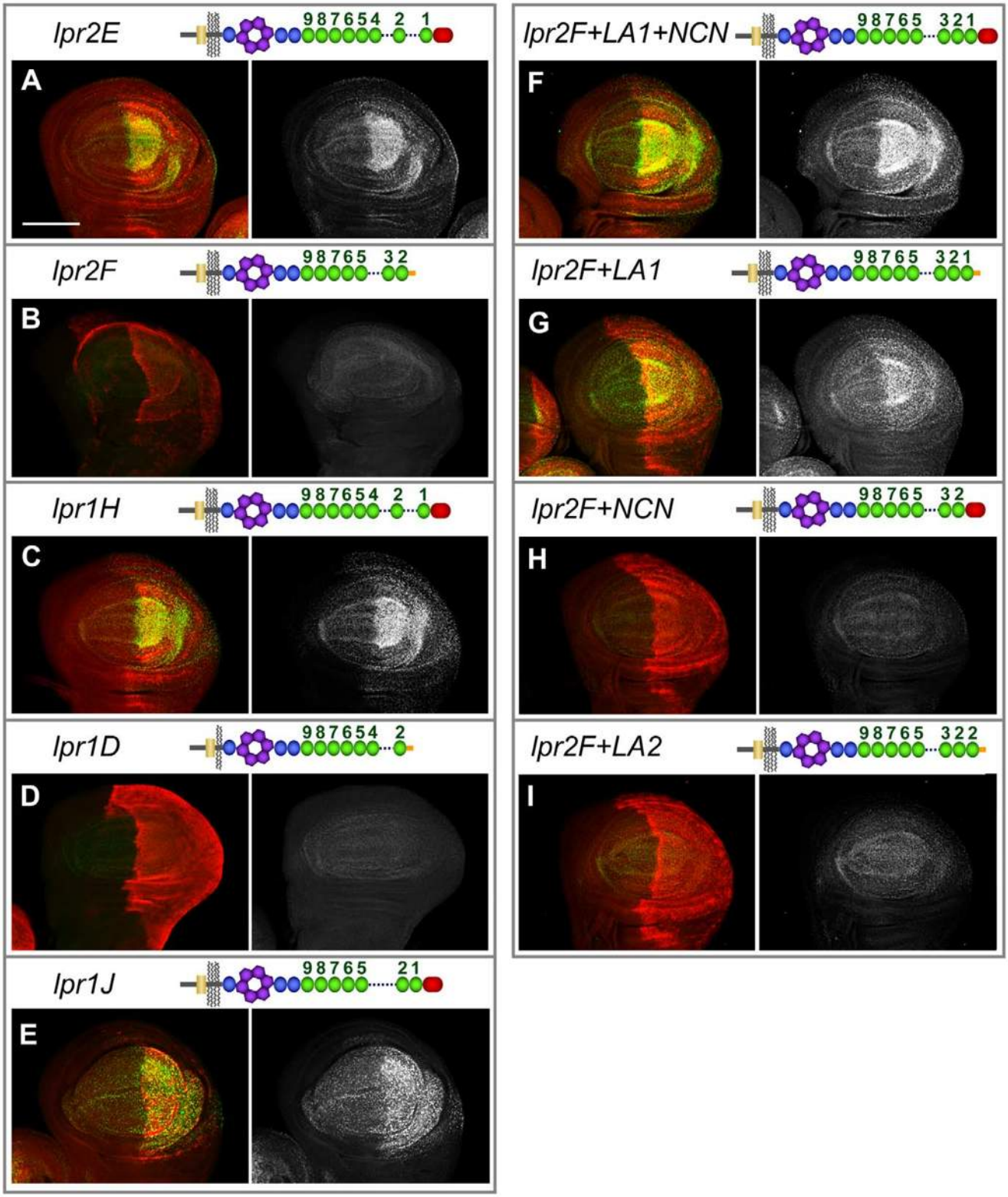

Figure 4. Uptake of neutral lipids is mediated by a subset of *lpr1* and *lpr2* isoforms. (A–I) Wing imaginal discs of *Df(3R)lpr1/2* genotype in which the indicated *lpr1* and *lpr2* isoforms and chimeras were overexpressed in the posterior compartment using the *en-gal4* driver. The relevant protein domains of the overexpressed isoforms are depicted in the drawings, which follow the code shown in Figure 1. Neutral lipids are shown in green and in grey in a separate channel. The overexpressed Lpr1 and Lpr2 proteins were detected by immunostaining using an antibody that recognizes the HA tag except in panel D in which α-Lpr1 was used. Lpr2E (A), Lpr1H (C), Lpr1J (E), Lpr2F+LA1+NCN (F) and Lpr2F+LA1 (G) proteins rescued lipid uptake in the posterior compartment whereas Lpr2F (B), Lpr1D (D), Lpr2F+NCN (H) and Lpr2F+LA2 (I) did not. Note that the presence of LA-1 defines the isoform ability to rescue neutral lipid uptake. Scale bar: 100 μm. All panels are shown at the same magnification.
doi:10.1371/journal.pgen.1001297.g004

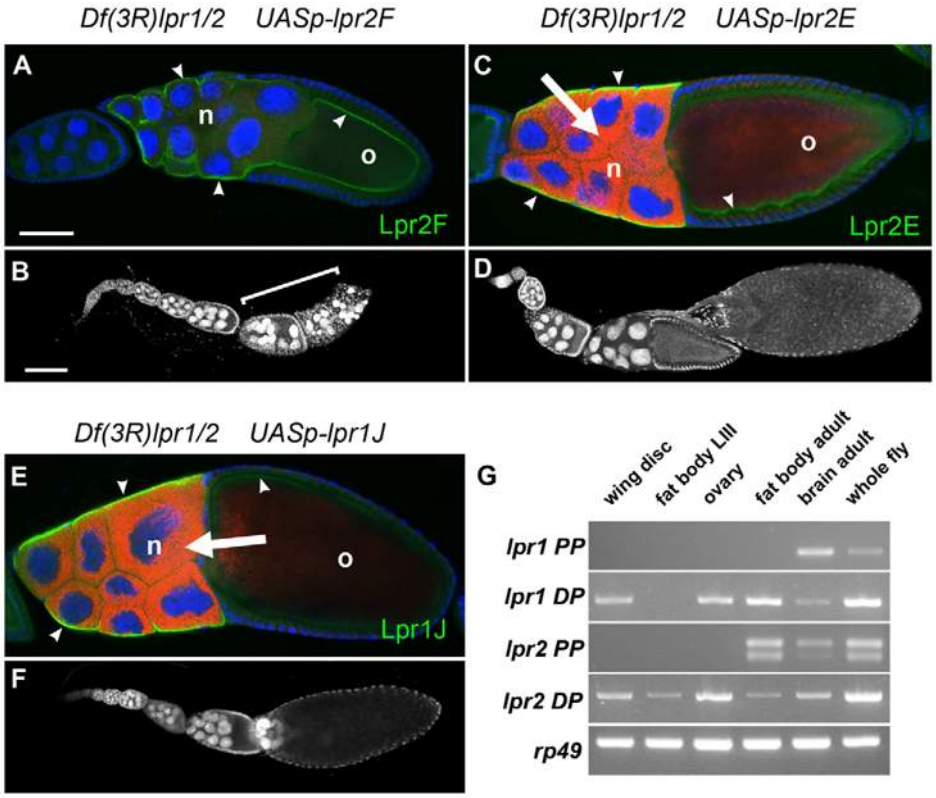

Figure 5. Germ-line expression of Lpr1J or Lpr2E rescues the oogenesis phenotypes of *lpr1*, *lpr2*$^{-}$ double mutant females. (A–F) *Df(3R)lpr1/2* egg chambers overexpressing the lipid uptake-defective *UASp-lpr2F* isoform (A–B) or the lipid uptake-promoting *UASp-lpr2E* (C–D) or *UASp-lpr1J* (E–F) isoforms in the germ-line driven by *V32-gal4*. (A,C,E) Lpr2F (A), Lpr2E (C) and Lpr1J (E) proteins were detected in the nurse cells (n) and oocyte (o) membranes using an α-HA antibody (arrowheads, shown in green). Egg chambers were stained with the lipophilic nile red dye (red) and DAPI (blue) to mark nuclei. (B, D, F) Ovarioles containing multiple egg chambers stained with DAPI. Several degenerating egg chambers are labeled with a bracket in (B). Note that germ-line specific expression of *UASp-lpr2E* and *UASp-lpr1J* but not of *UASp-lpr2F* induced accumulation of neutral lipids in nurse cells (arrows in C and E) and rescued mid-oogenesis degeneration (D and F, compare also with the wild-type and *Df(3R)lpr1/2* egg chambers in Figure 2). (G) Semiquantitative RT-PCR showing the relative abundance of *lpr1* and *lpr2* transcripts in several tissues, as indicated (wing imaginal discs, third instar larva fat body, ovary, adult fat body, adult brain and whole female fly). The oligo pairs used discriminated between isoforms transcribed from the proximal promoter (PP) and from distal promoter (DP). Analysis of ribosomal protein *rp49* transcription was included as a control. Scale bars: (A, C and E) 50 μm, (B, D and F) 100 μm.
doi:10.1371/journal.pgen.1001297.g005

However, our finding that lipophorin receptors have non-autonomous activity appears to be in conflict with this simple hypothesis, prompting us to test the requirement of endocytosis for lipophorin receptor-mediated lipid uptake. We took advantage of the fact that the *Drosophila* oocyte is a well characterized model of endocytosis, and importantly, that the endocytic pathway can be blocked in the oocyte and nurse cells without affecting their survival [29,30]. We generated germ-line clones of a null *rab5* mutation, an essential mediator of endocytic vesicle formation and maturation [31]. As previously reported, *rab5*^{2} mutant oocytes were unable to accumulate yolk proteins, demonstrating that the endocytic pathway was blocked [29,30] (Figure 6G', compare to 6F'). More importantly, *rab5*^{2} mutant egg chambers showed a normal accumulation of intracellular lipid droplets, indicating that the endocytosis of lipophorins is not required for neutral lipid uptake during vitellogenesis (Figure 6G, compare to 6F). Similarly, the AP-2 adaptor complex is not required for neutral lipid uptake (Figure S6 and Text S1). Together, these results suggest that in *Drosophila*, the neutral lipid uptake promoting activity of lipophorin receptors occurs extracellularly and that the targeting of lipophorins to lysosomes for their catabolic degradation is not required. In this scenario, a possible mechanism for lipophorin receptors to promote the uptake of neutral lipids would be by stabilizing lipophorins at the extracellular matrix. We tested this hypothesis by examining the extracellular distribution of lipophorins in *Df(3R)lpr1/2* imaginal discs that overexpressed *UAS-lpr2E* in the posterior compartment. We observed increased accumulation of extracellular lipophorins at the basolateral membranes of cells expressing Lpr2E (Figure 7A, 7B, arrows). In contrast, similar expression of the lipid uptake-defective Lpr2F isoform had no visible effect on the extracellular distribution of lipophorin (Figure 7C, 7D). Similar results were obtained overexpressing UAS-lpr2E and UAS-lpr2F with additional gal4 drivers (Figure S7).

Discussion

Over the past decade, *Drosophila* has become a prominent model organism for the study of lipid metabolism. Aspects ranging from the composition and regulation of lipid droplets, to the developmental control of adipose tissue differentiation or to the hormonal regulation of lipid storage and mobilization have revealed multiple parallels between *Drosophila* and mammals [3,32]. Moreover, large scale genetic screens in *Drosophila* have identified novel genes and pathways involved in energy homeostasis, some of which are conserved in mammals [32–36]. In this

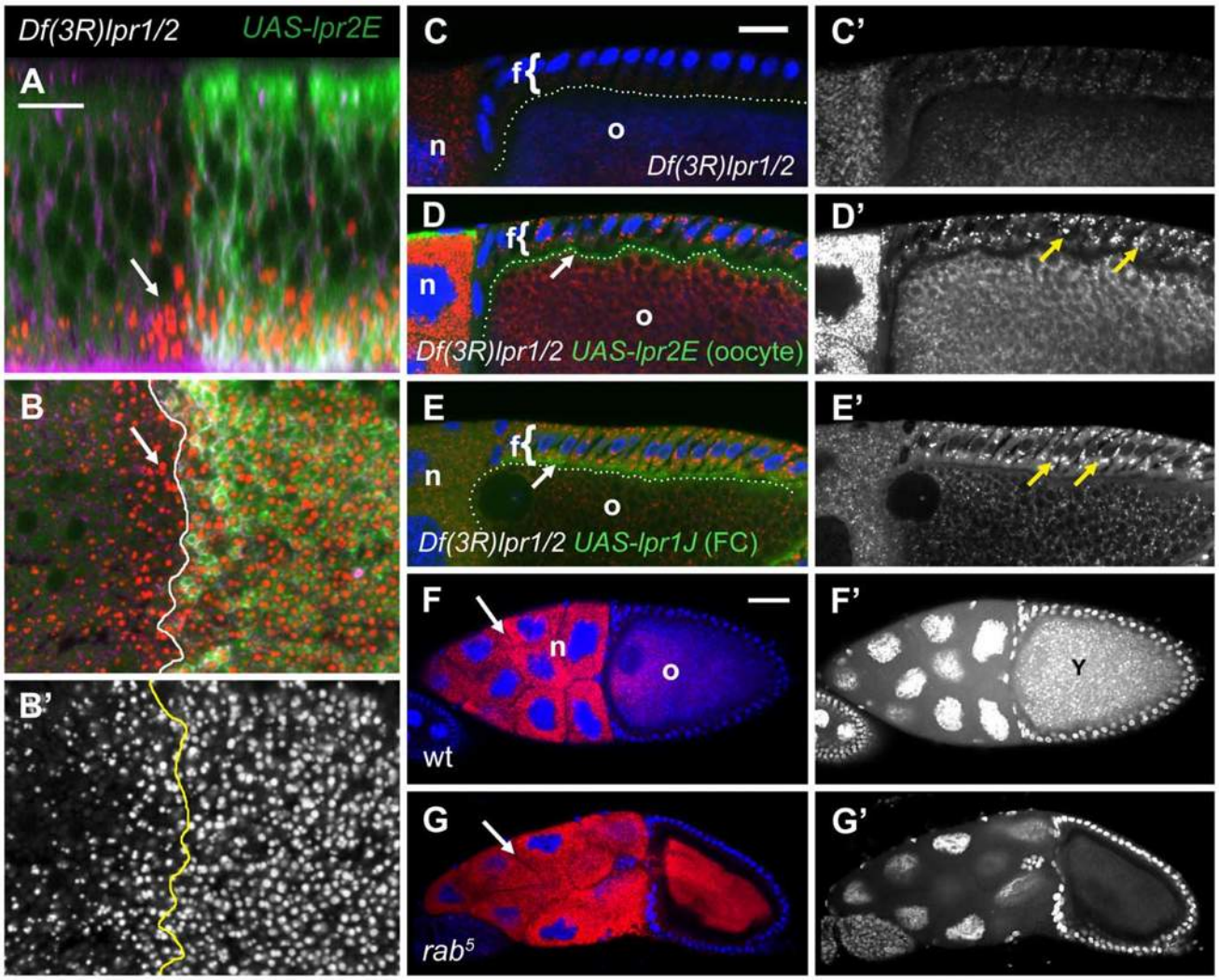

Figure 6. Neutral lipid uptake does not require endocytosis. (A–B) Wing imaginal disc of *Df(3R)lpr1/2* genotype expressing *UAS-lpr2E* in the posterior compartment driven by *en-gal4*. Neutral lipids were revealed by nile red staining (red). Lpr2E distribution was detected with α-HA antibody (green). Lipophorin distribution is shown in magenta to mark cell outlines. The wing imaginal disc is shown in a cross-section in (A), with the apical side at the top and the basal at the bottom. A basal section of the same disc is shown in (B). Note that Lpr2E expressing cells and two rows of adjacent non-expressing anterior cells (arrows) accumulate high levels of lipid droplets in a basal location. A line marks the limit of Lpr2E expression. Nile red staining is also shown in a separate panel (B'). (C–E) Detail of the somatic follicle epithelium (f) wrapping around the oocyte (o) in a stage 10 egg chamber dissected from a *Df(3R)lpr1/2* female (C) and similar *Df(3R)lpr1/2* mutant egg chambers overexpressing *UASp-lpr2E* in the germ-line driven by *V32-gal4* (D) or *UAS-lpr1J* in the follicular epithelium driven by *CY2-gal4* (E). Lpr2E and Lpr1J were detected with an α-HA antibody (green). The oocyte membrane was marked with a dotted line. Overexpressed proteins accumulated at the oocyte membrane (arrow in D) and at the apical region of the follicle cells (arrow in E). DAPI marks the cell nuclei (blue). Lipids are shown in grey as a separate channel (C', D' and E'). Note that expression of *UASp-lpr2E* in the nurse cells and oocyte induces an autonomous increase in lipid accumulation in these cells and also a non-autonomous rescue in the adjacent follicular epithelium (yellow arrows in D'). Expression of Lpr1J in the follicular epithelium rescues lipid accumulation in these cells to a similar extent (yellow arrows in E'). Note that the *Df(3R)lpr1/2* egg chamber shown in (C) was dissected from young females in which a few egg chambers from each ovary escaped mid oogenesis degeneration. (F–G) Egg chambers stained with the lipophilic dye nile red (red) and DAPI (blue) to mark cell nuclei. (F) Wild-type genotype. Note the accumulation of lipids (arrow) in the nurse cells (n) and the auto-fluorescence of yolk proteins (Y) (in F') in the DAPI channel within the oocyte (o). (G) *rab*^{5} mutant egg chamber. Lipids accumulate in the nurse cells (arrow) similarly to the wild-type but no yolk proteins are present in the oocyte (G'), confirming that endocytosis is blocked in the *rab*^{5} genetic background. Scale bars: 10 μm (A–B), 20 μm (C–E), 100 μm (F–G).
doi:10.1371/journal.pgen.1001297.g006

context, we have studied an aspect of lipid metabolism that was largely unknown in *Drosophila*: the cellular uptake of neutral lipids mediated by the lipophorin receptors.

The *Drosophila* genome contains two closely related genes (*lpr1* and *lpr2*, Figure 1A) homologous to other described lipophorin receptors in insects like locust, mosquitoes, cockroaches, silkworm, wax moth or bees [14,37–41]. Insect lipophorin receptors were first isolated because of their homology to the mammalian LDLR and subsequently shown to be involved in insect lipid metabolism. In particular, the locust Lipophorin Receptor, by far the best characterized member of the family, was able to induce the endocytic uptake of labeled lipophorins when expressed in mammalian cells [42]. Moreover, it was required for the endocytosis of lipophorins by locust fat body cells [15,16]. Here, we generated several novel mutations in *Drosophila* which disrupted *lpr1*, *lpr2* and, in view of a possible functional redundancy between

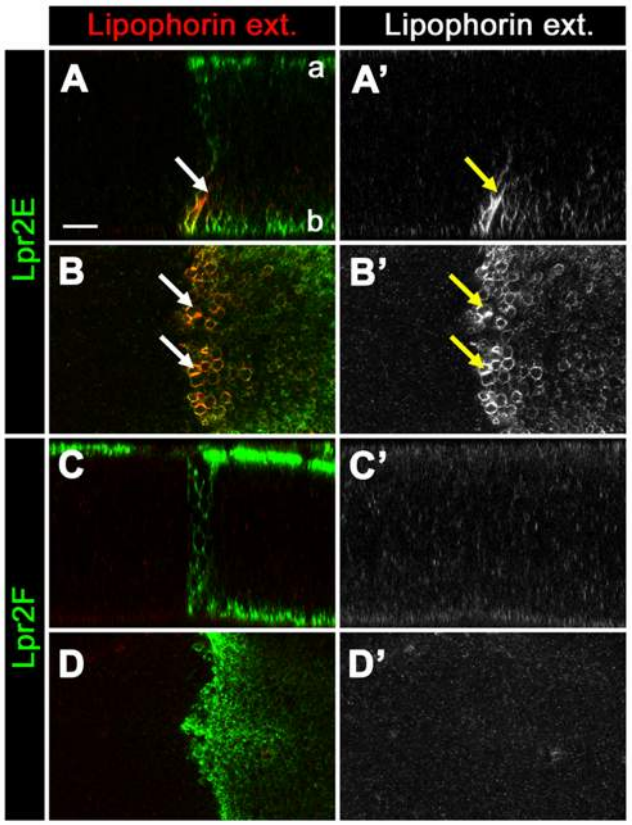

Figure 7. Lpr2E stabilizes lipophorins in the extracellular space. (A–D) *Df(3R)lpr1/2* wing imaginal discs overexpressing the lipid uptake-promoting *UAS-lpr2E* isoform (A–B) or the lipid uptake-defective *UAS-lpr2F* isoform (C–D) in the posterior compartment driven by *en-gal4,* shown in green. A modified immunostaining protocol was used to detect extracellular lipophorin (red, also shown in a separate panel in grey). (A, C) Optical cross-sections. Apical (a) and basal (b) sides as indicated. (B, D) Optical basal section. Cells overexpressing Lpr2E displayed increased accumulation of extracellular lipophorins at basolateral membranes near the basal side of the imaginal disc (arrows in A and B). The accumulation was more prominent near the antero-posterior compartment boundary, a region that also displayed higher Lpr2E protein levels. No noticeable changes in extracellular lipophorin were detected in cells overexpressing *UAS-lpr2F* (C–D). Scale bar: 10 μm. All panels are shown at the same magnification.
doi:10.1371/journal.pgen.1001297.g007

the two receptors, we also generated a deficiency that affects both genes simultaneously (*Df(3R)lpr1/2*), representing a null mutation for lipophorin receptor function (Figure 1A). Despite the critical role lipophorins play in lipid transport in insects [8,17] and the embryonic lethal phenotype of a null mutation in the single *Drosophila apolipophorin* gene [11], complete disruption of both *Drosophila* lipophorin receptors does not affect the viability of flies. Moreover, we did not detect any significant change in total body TAG content when we compared animals with mutations in *lpr1*, *lpr2* or the double mutant with their isogenic controls (Figure S4A–S4C). Moreover, the fat body cells of mutant and control animals were indistinguishable, containing similar number of lipid droplets and of equivalent sizes (Figure S4G–S4J). The rate of lipid mobilization under starvation conditions was also unaffected in *lpr1* and *lpr2* mutants (Figure S4D–S4F). Taken together, these results clearly demonstrated that *Drosophila* lipophorin receptors are not essential for the storage of TAG in the fat body or for its mobilization. Despite this lack of a requirement, we detected *lpr1* and *lpr2* expression in the adult fat body (Figure 5G and Figure S2C), and lipophorin receptors have been identified in the fat body of other insects [14,39–41,43,44]. Thus, the lipophorin receptors probably have functions in the fat body that are unrelated to the uptake of neutral lipids. Significantly, it has recently been reported that *lpr2* is involved in immune response in *Drosophila* as a regulator of the serpin Necrotic metabolism [45]. In addition, it was shown in microarray experiments that *lpr2* transcription changes upon immune challenge [46]. Since the fat body is a key immunological organ in the fly [47], it is possible that *lpr2* expression in this tissue is related to immunity.

We have shown that *lpr1* and *lpr2* have a key role in neutral lipid uptake in two *Drosophila* organs: the imaginal disc and the ovaries. In both cases, they are required to attain high levels of intracellular TAG. *lpr1* and *lpr2* are expressed in the wing pouch region of wing imaginal discs and mediate the uptake of neutral lipids by these cells (Figure 3). Another protein involved in lipid storage as a component of lipid droplets, the perilipin-like protein Lipid storage droplet-2 (Lsd-2), is also preferentially expressed and required in the wing pouch region for the accumulation of intracellular lipid droplets [26]. Thus, lipid accumulation in this region of the disc appears to be regulated at multiple levels. Unfortunately, the functional relevance of this lipid accumulation is still unknown.

Our results indicate that *lpr1* and *lpr2* genes are transcribed as multiple isoforms each (Figure 1B) with dramatically different properties. Only those isoforms transcribed from the distal promoters and containing the LA-1 module mediate lipid uptake. Similarly, the *lipophorin receptor* gene from the mosquito *Aedes aegypti* has been shown to be translated into fat body and oocyte specific isoforms from two alternative promoters [48]. Several members of the mammalian LDLR family are similarly processed by alternative splicing. Variations in the O-glycosylation region and the LA domains in mammalian VLDLR and ApoER2 have been related to differential sensitivity to proteolytic processing by gamma-secretases [49,50] and to differential ligand binding [51,52], respectively. Thus, the multiple *lpr1* and *lpr2* isoforms might have different ligand binding and/or stability properties, allowing these receptors to be involved in processes as diverse as neutral lipid uptake, regulation of the immune system [45] and regulation of neurite outgrowth [53].

Lipophorin receptors function during oogenesis

During vitellogenesis, the nurse cells and the oocyte grow rapidly accumulating large amounts of yolk proteins and lipids from the hemolymph over approximately 18 hours [21,54]. Work from the Mahowald lab has shown that Yolkless, an LDLR family protein, mediates the endocytic uptake of yolk proteins in *Drosophila* [22,23]. Here we demonstrate that a different receptor type, the lipophorin receptor, is essential for the uptake of neutral lipids during vitellogenesis (Figure 2). This is clearly shown in *Df(3R)lpr2* females and in double mutant *lpr1*$^{-}$, *lpr2*$^{-}$germ-line clones. In both cases, the mutant egg chambers accumulate low levels of neutral lipids (Figure 2J, 2M and Figure S3A). In addition to impaired lipid uptake during vitellogenesis, we observed a second phenotype in *Df(3R)lpr1/2* double mutant females, where most of the egg chambers degenerated at mid-oogenesis (Figure 2O and Figure S3B). A simple explanation for this phenotype would be that degeneration was triggered by the low lipid content of *Df(3R)lpr1/2* egg chambers. In fact, it is known that multiple challenges like starvation, extreme temperatures or chemical treatments, trigger a mid-oogenesis checkpoint and induce apoptosis at this stage [24]. Significantly, flies with a mutation in the gene *midway*, which encodes an acyl coenzyme A: diacylglycerol acyltransferase required for the synthesis of TAG, were

described to have severely reduced levels of neutral lipids in the germ-line and displayed apoptosis at mid oogenesis, thus paralleling the *Df(3R)lpr1/2* phenotype [55]. However, it was difficult to fully attribute degeneration to low lipid levels as we observed some experimental conditions which resulted in egg chambers with very low levels of neutral lipids but that did not undergo degeneration. In particular, in *Df(3R)lpr1/2* germ-line clones degeneration was absent even though the neutral lipid content of the egg chambers was low (Figure 2M). Similarly, expression of *UAS-lpr1J* exclusively in the follicle cells of *Df(3R)lpr1/2* females abolished egg chamber degeneration even though neutral lipid accumulation in the nurse cells and oocytes was low (Figure 6E and not shown). These experiments suggest that the lipophorin receptors might have an additional function in the follicle cells which is necessary to avoid egg chamber degeneration. Accordingly, we detected *lpr1* expression in the follicular epithelium (Figure 2A, inset). In this direction, it has recently been described that blocking the nutrient sensing TOR pathway in follicle cells induced apoptosis at mid oogenesis [56]. Thus, Lpr1 could be required to maintain elevated levels of TOR activity in follicle cells. In interpreting these results, we should also consider the non-autonomous effects of lipophorin receptors. We have shown that expression of *UAS-lpr2E* exclusively in the oocyte and nurse cells increases lipid uptake in the follicle cells (Figure 6D), which could potentially impact on their nutritional status and restore their putative anti-apoptotic activity. Conversely, expression of the transgene in the follicle cells might slightly increase lipid uptake by the oocyte and nurse cells, even though we have been unable to detect this effect (Figure 6E), and provide enough lipids to bypass the mid-oogenesis checkpoint. More studies will be required to assess the role of the lipophorin receptors in the follicular epithelium.

A speculative molecular model for lipid uptake mediated by the lipophorin receptors

Drosophila Lpr1 and Lpr2 are bona fide members of the LDLR family, sharing a similar organization of proteins domains with the human LDLR, ApoER2 and VLDLR. The human LDLR is the archetypical endocytic receptor. It is expressed in the liver where it mediates the endocytosis of cholesterol-rich LDL, regulating LDL concentration in serum. Endocytosis of LDL results in the catabolic processing of both, the lipidic and proteic moieties of LDL in lysosomes [13]. Other members of the LDLR family are also well known endocytic receptors with a broad variety of ligands [28,57]. *Drosophila* lipophorin receptors can also mediate endocytosis of their ligands. It has recently been reported that Lpr1 is expressed in garland cells and pericardial athrocytes where it is critical for the endocytic clearance of serpin/protease complexes from the hemolymph, thus regulating the innate immune response [45]. Overexpression of Lpr1 and Lpr2 in imaginal discs also induced the endocytosis of lipophorins, which colocalized with endocytic markers [11,27]. Similarly, the locust lipophorin receptor mediated lipophorin endocytosis in the fat body and in cell culture [14–16]. Despite this well documented endocytic activity of LDLRs, our data demonstrates that neutral lipid uptake mediated by *Drosophila* lipophorin receptors does not require the endocytosis of lipophorin particles. Three lines of evidence support this conclusion: (1) Blocking endocytosis did not affect lipid uptake in the egg chambers (Figure 6G and Figure S6); (2) overexpression of Lpr2E in groups of imaginal disc cells induced lipid uptake both in cells expressing the receptor and in a 1–2 cell diameter region of adjacent cells (Figure 6A, 6B, and Figure S5C, S5D) and (3) expression of Lpr2E in the oocyte and nurse cells promoted lipid uptake in the adjacent, somatic follicular epithelium (Figure 6D). Our results also indicate that Lpr2E is able to locally increase the concentration of lipophorins in the extracellular space (Figure 7A, 7B and Figure S7B, S7D, S7F). Taking into account this data, we propose the following model for lipophorin receptor-mediated neutral lipid uptake: lipophorin receptors interact with lipophorins at the cell surface and promote the extracellular hydrolysis of their DAG core by facilitating the activity of an as-yet-unidentified lipase, associated with the extracellular matrix. The free fatty acids generated during DAG hydrolysis could diffuse a few cell diameters away before being captured by cells, explaining why lipophorin receptors can promote lipid uptake non-autonomously. Significantly, physiological data obtained from studies of flight muscles and oocytes in insects indicated that lipid uptake mostly occurs without the concomitant degradation of the apolipophorin (for reviews, see [54,58]), which is consistent with our hypothesis. Moreover, a lipophorin-specific lipase activity associated with muscle and oocyte cell membranes was detected [54,58]. Our model offers a possible explanation to understand why only a subset of *lpr1* and *lpr2* isoforms mediates lipid uptake, whereby only the lipid-uptake promoting isoforms can stabilize lipophorins in the extracellular matrix (Figure 7 and Figure S7). Alternatively, if lipophorin receptors must interact with both, a lipophorin particle and a lipase to generate a ternary complex and facilitate lipolysis, then the lipid uptake-defective isoforms might lack the ability to interact with the lipase. Identification of such putative lipase(s) will be necessary to test this hypothesis. The proposed model displays a number of resemblances to the lipolytic processing of triglyceride-rich lipoproteins in the microvascular endothelium of adipose tissue, heart and striated muscles in mammals. Circulating triglyceride-rich lipoproteins, chylomicrons from the intestine and VLDL synthesized by the liver, reach the capillary endothelium where they interact with lipoprotein lipase at the luminal surface. Lipoprotein lipase is essential for the lipolytic processing of chylomicrons and VLDL, generating non-esterified fatty acids from the TAG fraction of lipoproteins. The free fatty acids are then transported to the underlying adipocytes and myocytes by specific transporters such as CD-36. Once inside these cells they are re-esterified into newly synthesized TAG stores or enter the β-oxidation cycle (for a recent review, see [59]). Recent data indicated that the extracellular lipolysis of TAG-rich lipoproteins is strongly potentiated by the endothelial protein GPIHBP1. This protein is essential for the transcytosis of lipoprotein lipase from the basolateral to the apical capillary endothelial surface [60]. In addition, it has been suggested that it may facilitate lipolysis by simultaneously interacting with lipoprotein lipase and chylomicrons in the luminal surface of capillaries, providing a molecular platform for lipolysis to occur [61]. In agreement with this essential functions, *Gpihbp1*-deficient mice manifested severe hyperchylomicronemia [61]. The VLDLR, which is also expressed at the capillary endothelium, seems to participate in the lipolytic processing of TAG-rich lipoproteins in similar ways. The VLDLR can mediate the transcytosis of lipoprotein lipase across cultured endothelial cells [62] and interacts with both, lipoprotein lipase and ApoE containing TAG-rich lipoproteins, potentially tethering them to the endothelium surface and thus promoting the action of lipoprotein lipase (for a review, see [63]). These potential functions were supported by the phenotype of vldlr^{-} mice, which showed delayed clearance of TAG-rich lipoproteins after a meal [64] and increased plasma TAG levels under a high fat diet [65] but normal lipoprotein profiles under regular feeding conditions [66]. Unfortunately, these weak phenotypes have hampered the elucidation of the precise roles that VLDLR plays during the processing of TAG-rich lipoproteins in vivo. We propose that in *Drosophila*, lipophorin

receptors have an activity similar to the bridging role proposed for GPIHBP1 and VLDLR in mammals, bringing lipophorins and a putative lipophorin-specific lipase into close contact on the cell surface and promoting in this way the lipolysis of lipophorins. We speculate that during evolution, a protein related to VLDLR had a critical role in promoting the extracellular hydrolysis of lipoproteins. In insects, this function is carried out by the lipophorin receptors whereas in mammals, GPIHBP1 appears to have taken most of this function, with VLDLR retaining a minor role. Our data supports an ancient function for the LDLR family in promoting the extracellular lipolytic processing of lipoproteins.

Methods

Genetics

Generation of deficiencies in the *lpr1-lpr2* genomic region: The three deficiencies used in this work were created by flipase-mediated interchromosomal recombination between the following pairs of FRT-containing transposon insertions: *Df(3R)lpr1*: P{XP}d03066 and P{XP}d10508 to generate a 19.7 Kb deletion; *Df(3R)lpr2*: PBac{RB}e00374 and PBac{WH}f03030 to generate a 29.7 Kb deletion; and *Df(3R)lpr1/2*: PBac{RB}e00374 and P{XP}d10508 to generate a 49,7 Kb deletion [67,68]. The deficiency breakpoints were checked by PCR using appropriate primers flanking the predicted breakpoints.

To generate *Df(3R)lpr1/2* clones in the female germ-line, *Df(3R)lpr1/2* was recombined with *FRT82B* [69] using standard genetic techniques. Females of the genotype: *y,w,hs-flp*; *FRT82B*, *Df(3R)lpr1/2/FRT82B,ovoD1* were heat-shocked for one hour at 37°C several times during larval stages. The resulting adult females were fed yeast over two days before their ovaries were dissected and processed for immunostaining. To generate rab^5 germ-line clones, females of the genotype *y,w,hs-flp*; rab^5*,FRT40A/ovoD1,FRT40A* were similarly treated. The rab^5*,FRT40A/CyO* stock was obtained from Antoine Guichet [30]. *FRT82B,ovoD1* and *ovoD1,FRT40A* chromosomes were described in [70].

To quantify egg hatching rates, less than a week old adults of the following genotypes: wild-type Oregon R, *w*;*Df(3R)lpr1/TM6* and *w*;*Df(3R)lpr2/TM6* were kept on abundant yeast paste for two days. Homozygous females were selected and allowed to lay eggs in apple plates for periods of 4 hours. About 200 eggs were individually placed in agar plates and incubated at 25°C for 48 hours. The number of empty egg shells and non-eclosed eggs was quantified.

Isolation and characterization of *lpr1* and *lpr2* isoforms and RT-PCR

Some of the cDNAs corresponding to *lpr1* and *lpr2* isoforms used in this work were isolated and sequenced by the Berkeley *Drosophila* Genome Project [19]. In particular, we used the following full length cDNAs: Lpr1D (RE14223), Lpr1H (LD21010), Lpr1J(RE40649), Lpr2F (GH26833) and Lpr2E (LD11117). To identify additional isoforms, total RNA was isolated from whole adult male flies and specific tissues -wing imaginal discs, ovaries, adult brain and adult fat body- using Trizol reagent (Invitrogen). 1 µg RNA for each sample was retrotranscribed using random primer and Transcriptor Reverse Transcriptase (Roche). The obtained cDNA libraries were PCR amplified using four oligo pairs which specifically amplified the complete coding regions corresponding to *lpr1* and *lpr2* genes transcribed from the proximal and distal promoters. The PCR products were directly cloned into pGEM-T (Promega) or alternatively, used for a second nested PCR reaction before purification and cloning of the products. 33 isolated cDNAs were genotyped by PCR and selected clones were also verified by sequencing to unambiguously define their specific combination of exons. Signal peptides were predicted using the SignalP 3.0 Server [71] and Predisi [20].

RT-PCR was used to examine *lpr1* and *lpr2* transcription in whole adult flies, larval fat body, wing imaginal discs, ovaries, adult brains and adult fat body. For adult fat body preparation, abdomen carcasses were used which primarily contained fat body. However, contaminating tissues including oenocytes, dorsal vessel, epidermis and muscle were also present in small quantities. Two oligo pairs were used for each gene, which specifically detected exons 2–3 (distal promoter isoforms; *lpr1*: attcggcaaatgctgcactgc and tgtgatccttgcagtccgcatc, *lpr2*: accacccagtcagagttaacaac and tgtggtccgggcaatccgagga) and exons 4–5 (proximal promoter isoforms; *lpr1*: cgaacctctcaaccaaacggat and gccagaacgcgaaaactttgg, lpr2: aagaaacggacgtgtgtgctc and ccaatccgacgactctggag). In addition, oligo pairs for the ribosomal protein gene *rp49* were used as control (gaccatccgcccagcatacaggc and gagaacgcaggcgaccgttgg). The oligos were designed to amplify a region encompassing an intron to distinguish cDNA products from genomic DNA products. A rough estimate of relative expression levels in the different tissues was obtained by comparing the PCR products at 20 and 30 cycles to avoid reaching an amplification plateau.

Immunostaining, in situ hybridization, and neutral lipids visualization

To generate α-Lpr1 and α-Lpr2 antibodies, DNA fragments containing the complete Lpr1 or Lpr2 intracellular domains were amplified by PCR from *lpr1* cDNA RE38584 and *lpr2* cDNA GH26833. The fidelity of the amplification was checked by sequencing and the fragments were cloned in-frame with the 6xHis tag present in the bacterial expression vector pET14b. Protein expression was induced in *E. coli*. The Lpr1 fragment was purified under denaturing conditions by immobilized metal affinity chromatography (IMAC) and dialyzed to remove urea. The protein precipitated during dialysis and the precipitate was used to immunize guinea pigs. Lpr2 fragment was purified from the soluble fraction by IMAC. Antibodies were raised in guinea pigs by Cocalico biologicals, Inc. Other antibodies used were: rabbit anti-apolipophorin 1:500 [10]; rat anti-HA 1:500 (Roche); and the dye DAPI to label nuclei.

For immunostaining, imaginal discs and ovaries were dissected and fixed for 20 minutes with 4% formaldehyde dissolved in PBS (PP) at room temperature, followed by a second fixation in PP plus 0.1% triton X-100. Tissues were extensively washed for 1 hour in PBS containing 0.3% triton X-100 (PBT) and blocked in 1% BSA dissolved in PBT for another hour. After incubation with the primary antibodies overnight at 4°C, tissues were extensively washed three times for a total of one hour in PBT and incubated with the fluorescent secondary antibodies (alexa-fluor conjugates from Invitrogen) for two hours (imaginal discs) or overnight (ovaries). After washing, tissues were mounted in vectashield media.

To detect extracellular lipophorins in imaginal discs, we used an extracellular staining protocol modified from [72]. Imaginal discs were dissected and accumulated in Sf-900 cell culture media (Invitrogen) on ice. They were incubated with α-Lipophorin antibody diluted 1:100 in cell culture media for 30 minutes with constant rocking and washed four times for a total of 30 minutes with PBS. Incubations and washes were done at 4°C to inhibit antibody endocytosis. Imaginal discs were then fixed with PP and from this point on processed following the standard immunostaining procedure.

Neutral lipids in imaginal discs and ovaries were visualized by nile red staining. Fixed tissues were incubated with 0.002% nile

red diluted in PBT for 60 minutes and washed for 10 minutes in the same buffer without the dye. To prepare embryos for microscopy, we avoided the use of organic solvents that would otherwise extract neutral lipids. Thus, after removing the chorion with bleach, we fixed embryos with a heat treatment of 5 seconds at 90°C and devitelinized them by hand using a sharp needle. The embryos were then incubated with the nile red solution as above.

We analyzed the tissue distribution of *lpr1* and *lpr2* transcription by in situ hybridization using DIG-labeled antisense RNA probes. Some probes were specific to particular isoforms whereas others recognized all isoforms derived from *lpr1* or *lpr2*. They were prepared from the following DNA fragments: (1) All *lpr1* isoforms: a 594 base pair DNA fragment including 64 base pairs from the C-terminal coding region and part of the 3′UTR of cDNA RE14223. (2) All *lpr2* isoforms: a 581 base pair fragment including 91 base pairs from the C-terminal coding region of cDNA GH26833 and part of its 3′UTR. (3) *lpr1* isoforms transcribed from the distal promoter: a 413 base pair fragment derived from exons 1 and 2 of cDNA LD21010. (4) *lpr2* isoforms transcribed from the distal promoter: a 500 base pair fragment derived from exon 2 of cDNA LD11117. Since the two *lpr* genes are highly homologous, probes were designed from the most divergent regions to avoid cross-reactivity. Probes 1 and 2 were used in Figure 3E, 3F and probes 3 and 4 in Figure 2A, 2B. The in situ hybridization protocol was carried out according to [73]. To illustrate immunostaining and in situ data, representative images were selected from each experiment after analyzing a minimum of 10 individual imaginal discs or egg chambers from at least two independent experiments.

Transgene construction and overexpression experiments

A *UAS-lpr1D* transgene was made by cloning the complete coding sequence of *lpr1* cDNA RE14223 [74] into the pUAST plasmid [75]. *UAS-lpr1B, UAS-lpr1J, UAS-lpr2F* and *UAS-lpr2E* transgenes were obtained by first amplifying the complete corresponding coding regions by PCR using the following templates: LD21010, RE40649, GH26833 and LD11117 [74] respectively. The resulting fragments were fused to a C-terminal 3xHA tag and transferred to pUAST attB [76] to obtain transgenic flies by the integrase phiC31 based system [76]. This method allows for the integration of the transgenes into the same chromosomal location, minimizing positional effects on transcription. All pUAST attB transgenes used were inserted into the 22A landing site [76]. The pUAST or pUAST attB plasmids do not allow expression in the germ-line. Thus, for expression in oocytes and nurse cells we generated *UASp-lpr1J, UASp-lpr2F* and *UASp-lpr2E* using the plasmid pUASP [77]. The inserts are identical to *UAS-lpr1J, UAS-lpr2F* and *UAS-lpr2E* including the C-terminal 3xHA tag. To generate the *lpr2F-lpr2E* chimeras, a NotI site was first inserted after Leu30, located between the signal peptide and the LA-2 domain of lpr2F (GH26833) by directed mutagenesis, generating pAC-lpr2F-NotI. NotI flanked fragments containing LA1 (from Ser186 to Thr232) and LA2 (from Glu233 to Cys272) were generated by PCR using *lpr2E* cDNA LD11117 as template, subsequently cloned into the NotI site of pAC-lpr2F-NotI and transferred to pUAST attB to generate *UAS-lpr2F+LA1* and *UAS-lpr2F+LA2* respectively. *UAS-lpr2F+LA1+NCN* and *UAS-lpr2F+NCN* were similarly generated by replacing the Asp718 (located at the transcription start site)-NotI region of pAC-lpr2F-NotI vector by fragments containing *LA1+NCN* (from Met1 to Thr232) and *NCN* (from Met1 to Ile185) regions of lpr2E cDNA LD11117 obtained by PCR and flanked by Asp718 and NotI sites. In all cases, the limits of the protein domains coincided with exon boundaries. All chimeras also contain a C-terminal 3xHA tag.

En-Gal4, obtained from A. Martínez-Arias, was used to drive expression at the posterior compartment of wing imaginal discs, *V32-Gal4*, a gift from Daniel St Johnston, to drive expression at the germline, and *CY2-gal4* [78] to direct expression at the ovarian follicle cells.

Supporting Information

Figure S1 The LDLR family in *Drosophila*. Analysis of the *Drosophila* genome using Blast searches and manual annotation resulted in the identification of seven genes encoding transmembrane proteins containing the three protein domains that define the LDLR family: YWTD β-propellers, LA modules and EGF modules. The uncharacterized *Drosophila* genes CG42611, CG33087 and CG8909 are probable orthologs of mammalian Megalin, Lrp1/Lrp1b and Megf7 (also known as Lrp4) genes respectively. The double line in the eight β-propeller of CG33087 protein represents a post-transcriptional cleavage (our unpublished results) similar to the one described for mammalian Lrp1 protein. LA modules colored in light green are not present in all isoforms. Domain composition for the human VLDLR and the locust lipophorin receptor are shown for comparison.
Found at: doi:10.1371/journal.pgen.1001297.s001 (1.20 MB TIF)

Figure S2 Specificity of α-Lpr1 and α-Lpr2 antibodies. (A–B) Wild-type (A) and *Df(3R)lpr1* (B) embryos were immunostained with α-Lpr1 (green) and α-Salm (red), a oenocytes marker. Only wild-type oenocytes were stained with α-Lpr1. The α-Lpr1 channel is shown in (A'–B'). (C–D) Wild-type (C) and *Df(3R)lpr2* (D) adult fat body were immunostained with α-Lpr2 (green). Nuclei were stained with DAPI (blue) and cell outlines were revealed with phalloidin staining (red). Only wild-type fat body was stained with α-Lpr2. The α-Lpr2 channel is shown in (C'–D'). (E–F) Wild-type (E) and *Df(3R)lpr2* stage 10 egg chambers immunostained with α-Lpr2. Only the wild-type egg chamber shows staining. Scale bars: 10 μm (A–B), 50 μm (C–D) and 100 μm (E–F).
Found at: doi:10.1371/journal.pgen.1001297.s002 (3.88 MB TIF)

Figure S3 Oogenesis phenotypes. (A) Plot of individual data points of nile red fluorescence from stage 10 egg chambers of control (w), *Df(3R)lpr1* and *Df(3R)lpr2* genotypes, as indicated (n = 40). Mean values are marked by red lines. Nile red fluorescence of the nurse cells was quantitated using ImageJ software and shown as mean gray values (from 0, black to 255, white). Nuclei were excluded from the measurements as indicated by a dotted line in the second egg chamber. Note that in all three genotypes, data points have broad distributions, partially reflecting maturation degrees of stage 10 egg chambers. w and *Df(3R)lpr1* genotypes have similar distributions, whereas most of the *Df(3R)lpr2* egg chambers have low lipid content. Three egg chambers stained with nile red (yellow) and DAPI (blue) and quantitated as having 200, 130 and 60 nile red fluorescence arbitrary units are shown for reference. (B) Ratio of egg chambers at each vitellogenic stage for the indicated genotypes. Note that most *Df(3R)lpr1/2* egg chambers degenerate at stages 9–10. This explains the almost complete lack of post-stage 9 egg chambers in this genotype. Overexpression of *UASp-lpr2E* or *UASp-lpr1J* in the germ-line of *Df(3R)lpr1/2* females using the *V32-gal4* driver restores the distribution of egg chamber stages to wild-type.
Found at: doi:10.1371/journal.pgen.1001297.s003 (1.77 MB TIF)

Figure S4 *lpr1* and *lpr2* do not affect TAG storage or mobilization in the fat body. (A–C) TAG content of a cohort of adult fly males of the indicated genotypes (red line) was measured at the time of eclosion (0 days) and at 2 days intervals thereafter. For each experiment, a similar cohort of isogenic w^{1118} males was used as control (blue line). Both, mutant and control flies were kept

in the same bottle during the course of the experiment. No significant TAG content differences were observed between w^{1118} flies and any of the three genotypes tested. Evolution of TAG content with age is slightly different from experiment to experiment, probably because of uncontrollable differences in food quality and environmental conditions in each bottle. (D–F) TAG content of a cohort of adult males of the indicated genotypes (red line) kept under starvation conditions. At the start of the experiment (hour 0), the males were 10 days old and had been kept with abundant yeast paste until that time. At time 0, males were transferred to a bottle containing only water and no nutrients and TAG content was measured at 5 h intervals. Males of the isogenic stock w^{1118} were included as control in all experiments (blue line). Linear regression are shown as dotted lines. The control flies were kept in the same bottle as the experimental flies. Under these strict starvation conditions, TAG content diminishes steadily for about 30 hours, at which time flies start dying. No significant differences in the rate of lipid mobilization were observed between the control and any of the three genotypes analyzed. In all graphs, 5% intervals of confidence are shown. (G–J) Fat body tissue dissected from early third instar larvae or adult male abdomens of *Df(3R)lpr1/2* and *Df(3R)lpr1/2/+* genotypes as indicated, was stained with nile red (yellow) to reveal lipid droplets and counterstained with TOTO3 (blue). The amount and size of lipid droplets is not altered in $lpr1^{-}$, $lpr2^{-}$ double mutants. Scale bar: 50 μm (G–J, same magnification). (K) TAG content in the hemolymph of third instar larvae of the indicated genotypes. 5% confidence intervals are shown. No statistically significant differences were observed.
Found at: doi:10.1371/journal.pgen.1001297.s004 (2.25 MB TIF)

Figure S5 Lpr2E mediates non-autonomous lipid uptake in the wing imaginal disc. (A–D) Wing imaginal discs of *Df(3R)lpr1/2* genotype expressing the lipid uptake-defective isoform Lpr2F (A–B) and the lipid uptake-promoting isoform Lpr2E (C–D) in the dorsal compartment driven by *ap-gal4*. Neutral lipids were revealed by nile red staining (red). Lpr2F and Lpr2E were detected with α-HA antibody (green). Cell outlines are marked in blue by α-Lp. Wing imaginal discs are shown in cross-sections (A and C; a: apical, b: basal) and in subapical sections (B, D). Note that Lpr2E expressing cells and two-three rows of adjacent ventral cells (arrow in D) accumulate high levels of lipid droplets. Expression of Lpr2F does not rescue lipid uptake and is shown here as a control (A, B). White lines mark the limit of Lpr2F and Lpr2E expression. Nile red staining is shown in separate panels (B', D'). Scale bar: 10 μm. All panels shown at the same magnification.
Found at: doi:10.1371/journal.pgen.1001297.s005 (3.23 MB TIF)

Figure S6 The AP-2 complex is not required for the uptake of neutral lipids during vitellogenesis. Germ-line clones of the alleles AP-2α^{40-31} and AP-2σ^{KG0245} marked by the absence of GFP (green) in nurse cells (n), as indicated. Neutral lipids are shown in red and yolk proteins autofluorescence (Y) in blue. Accumulation of neutral lipids during vitellogenesis does not require the AP-2 adaptor complex. Endocytosis of yolk proteins also appears to be AP-2 independent. Scale bar: 100 μm.
Found at: doi:10.1371/journal.pgen.1001297.s006 (1.44 MB TIF)

Figure S7 Lpr2E overexpression stabilizes extracellular lipophorin. (A) Wild-type wing imaginal disc showing the distribution of extracellular lipophorin in red and grey in a separate panel. (B-G) Wing imaginal discs overexpressing *UAS-lpr2E* (B, D, F) or *UAS-lpr2F* (C, E, G) under the control of the *ptc-gal4* (B-C), *wg-gal4* (D–E) or *en-gal4* (F–G) drivers on a wild-type genetic background (B–E) or a *Df(3R)lpr1/2* background (F–G). Lpr2E and Lpr2F are shown in green. Extracellular lipophorin is shown in red and grey in a separate panel. Note that *UAS-lpr2E* expression increases extracellular lipophorin signal (B', D', F', arrows). Overexpression of *UAS-lpr2F* does not have this effect (C', E', G'). Scale bar: 100 μm.
Found at: doi:10.1371/journal.pgen.1001297.s007 (4.87 MB TIF)

Text S1 Supplementary methods. Triacylglycerol quatification and generation of AP-2 germ-line clones.
Found at: doi:10.1371/journal.pgen.1001297.s008 (0.03 MB DOC)

Acknowledgments

We are grateful to J. Modolell and S. Campuzano for their continuous support during this work. The initial studies were carried out at R. S. Manns laboratory at Columbia University. The outstanding technical help of John Edward Mejía and Eva Caminero has been invaluable. We thank S. Campuzano, J. Castelli-Gair Hombría, J. Modolell, M. Ruiz-Gómez, S. Sotillos, and members of the lab for suggestions; J. Modolell, MJ. García-García, S. Sotillos, and Z. Wang for critically reading the manuscript; D. Bilder, A. Guichet, D. St Johnston, T. Schüpbach, the Bloomington Stock Center, and The Exelixis Collection for flies; K. Kutty for antibodies; and the "*Drosophila* Microinjection Facility" from the "Consolider-Ingenio 2010 GESHAPE" for microinjections.

Author Contributions

Conceived and designed the experiments: EPP JC. Performed the experiments: EPP JC. Analyzed the data: EPP JC. Wrote the paper: JC.

References

1. Kopelman PG (2000) Obesity as a medical problem. Nature 404: 635–643.
2. Barsh GS, Schwartz MW (2002) Genetic approaches to studying energy balance: perception and integration. Nat Rev Genet 3: 589–600.
3. Baker KD, Thummel CS (2007) Diabetic larvae and obese flies-emerging studies of metabolism in Drosophila. Cell Metab 6: 257–266.
4. Bharucha KN (2009) The epicurean fly: using Drosophila melanogaster to study metabolism. Pediatr Res 65: 132–137.
5. Leopold P, Perrimon N (2007) Drosophila and the genetics of the internal milieu. Nature 450: 186–188.
6. Schlegel A, Stainier DYR (2007) Lessons from "lower" organisms: what worms, flies, and zebrafish can teach us about human energy metabolism. PLoS Genet 3: e199. doi:10.1371/journal.pgen.0030199.
7. Vance D, Vance J (2002) Biochemistry of lipids, lipoproteins and membranes; Vance D, Vance J, eds. Amsterdam: Elsevier Science.
8. Canavoso LE, Jouni ZE, Karnas KJ, Pennington JE, Wells MA (2001) Fat metabolism in insects. Annu Rev Nutr 21: 23–46.
9. Van der Horst DJ, Roosendaal SD, Rodenburg KW (2009) Circulatory lipid transport: lipoprotein assembly and function from an evolutionary perspective. Mol Cell Biochem 326: 105–119.
10. Kutty RK, Kutty G, Kambadur R, Duncan T, Koonin EV, et al. (1996) Molecular characterization and developmental expression of a retinoid- and fatty acid-binding glycoprotein from Drosophila. A putative lipophorin. J Biol Chem 271: 20641–20649.
11. Callejo A, Culi J, Guerrero I (2008) Patched, the receptor of Hedgehog, is a lipoprotein receptor. Proc Natl Acad Sci U S A 105: 912–917.
12. van der Horst DJ, van Hoof D, van Marrewijk WJ, Rodenburg KW (2002) Alternative lipid mobilization: the insect shuttle system. Mol Cell Biochem 239: 113–119.
13. Brown MS, Goldstein JL (1986) A receptor-mediated pathway for cholesterol homeostasis. Science 232: 34–47.
14. Dantuma NP, Potters M, De Winther MP, Tensen CP, Kooiman FP, et al. (1999) An insect homolog of the vertebrate very low density lipoprotein receptor mediates endocytosis of lipophorins. J Lipid Res 40: 973–978.
15. Van Hoof D, Rodenburg KW, van der Horst DJ (2003) Lipophorin receptor-mediated lipoprotein endocytosis in insect fat body cells. J Lipid Res 44: 1431–1440.
16. Van Hoof D, Rodenburg KW, Van der Horst DJ (2005) Receptor-mediated endocytosis and intracellular trafficking of lipoproteins and transferrin in insect cells. Insect Biochem Mol Biol 35: 117–128.

17. Rodenburg KW, Van der Horst DJ (2005) Lipoprotein-mediated lipid transport in insects: analogy to the mammalian lipid carrier system and novel concepts for the functioning of LDL receptor family members. Biochim Biophys Acta 1736: 10–29.
18. Schneider WJ, Nimpf J (2003) LDL receptor relatives at the crossroad of endocytosis and signaling. Cell Mol Life Sci 60: 892–903.
19. Stapleton M, Liao G, Brokstein P, Hong L, Carninci P, et al. (2002) The Drosophila gene collection: identification of putative full-length cDNAs for 70% of D. melanogaster genes. Genome Res 12: 1294–1300.
20. Hiller K, Grote A, Scheer M, Münch R, Jahn D (2004) PrediSi: prediction of signal peptides and their cleavage positions. Nucleic Acids Res 32: W375–379.
21. Spradling AC (1993) Developmental genetics of oogenesis. In: Bate M, Arias AM, eds. The Development of Drosophila melanogaster Cold Spring Harbor Laboratory Press. pp 1, 70.
22. Schonbaum CP, Lee S, Mahowald AP (1995) The Drosophila yolkless gene encodes a vitellogenin receptor belonging to the low density lipoprotein receptor superfamily. Proc Natl Acad Sci U S A 92: 1485–1489.
23. Schonbaum CP, Perrino JJ, Mahowald AP (2000) Regulation of the vitellogenin receptor during Drosophila melanogaster oogenesis. Mol Biol Cell 11: 511–521.
24. McCall K (2004) Eggs over easy: cell death in the Drosophila ovary. Dev Biol 274: 3–14.
25. Terashima J, Takaki K, Sakurai S, Bownes M (2005) Nutritional status affects 20-hydroxyecdysone concentration and progression of oogenesis in Drosophila melanogaster. J Endocrinol 187: 69–79.
26. Fauny JD, Silber J, Zider A (2005) Drosophila Lipid Storage Droplet 2 gene (Lsd-2) is expressed and controls lipid storage in wing imaginal discs. Dev Dyn 232: 725–732.
27. Khaliullina H, Panáková D, Eugster C, Riedel F, Carvalho M, et al. (2009) Patched regulates Smoothened trafficking using lipoprotein-derived lipids. Development 136: 4111–4121.
28. Strickland DK, Gonias SL, Argraves WS (2002) Diverse roles for the LDL receptor family. Trends Endocrinol Metab 13: 66–74.
29. Morrison HA, Dionne H, Rusten TE, Brech A, Fisher WW, et al. (2008) Regulation of early endosomal entry by the Drosophila tumor suppressors Rabenosyn and Vps45. Mol Biol Cell 19: 4167–4176.
30. Compagnon J, Gervais L, Roman MS, Chamot-Boeuf S, Guichet A (2009) Interplay between Rab5 and PtdIns(4,5)P2 controls early endocytosis in the Drosophila germline. J Cell Sci 122: 25–35.
31. Zerial M, McBride H (2001) Rab proteins as membrane organizers. Nat Rev Mol Cell Biol 2: 107–117.
32. Pospisilik JA, Schramek D, Schnidar H, Cronin SJF, Nehme NT, et al. (2010) Drosophila genome-wide obesity screen reveals hedgehog as a determinant of brown versus white adipose cell fate. Cell 140: 148–160.
33. Al-Anzi B, Sapin V, Waters C, Zinn K, Wyman RJ, et al. (2009) Obesity-blocking neurons in Drosophila. Neuron 63: 329–341.
34. Beller M, Sztalryd C, Southall N, Bell M, Jäckle H, et al. (2008) COPI complex is a regulator of lipid homeostasis. PLoS Biol 6: e292. doi:10.1371/journal.pbio.0060292.
35. Gronke S, Mildner A, Fellert S, Tennagels N, Petry S, et al. (2005) Brummer lipase is an evolutionary conserved fat storage regulator in Drosophila. Cell Metab 1: 323–330.
36. Guo Y, Walther TC, Rao M, Stuurman N, Goshima G, et al. (2008) Functional genomic screen reveals genes involved in lipid-droplet formation and utilization. Nature 453: 657–661.
37. Guidugli-Lazzarini KR, do Nascimento AM, Tanaka ED, Piulachs MD, Hartfelder K, et al. (2008) Expression analysis of putative vitellogenin and lipophorin receptors in honey bee (Apis mellifera L.) queens and workers. J Insect Physiol 54: 1138–1147.
38. Cheon HM, Seo SJ, Sun J, Sappington TW, Raikhel AS (2001) Molecular characterization of the VLDL receptor homolog mediating binding of lipophorin in oocyte of the mosquito Aedes aegypti. Insect Biochem Mol Biol 31: 753–760.
39. Ciudad L, Bellés X, Piulachs M (2007) Structural and RNAi characterization of the German cockroach lipophorin receptor, and the evolutionary relationships of lipoprotein receptors. BMC Mol Biol 8: 53.
40. Gopalapillai R, Kadono-Okuda K, Tsuchida K, Yamamoto K, Nohata J, et al. (2006) Lipophorin receptor of Bombyx mori: cDNA cloning, genomic structure, alternative splicing, and isolation of a new isoform. J Lipid Res 47: 1005–1013.
41. Lee CS, Han JH, Kim BS, Lee SM, Hwang JS, et al. (2003) Wax moth, Galleria mellonella, high density lipophorin receptor: alternative splicing, tissue-specific expression, and developmental regulation. Insect Biochem Mol Biol 33: 761–771.
42. Dantuma NP, Pijnenburg MA, Diederen JH, Van der Horst DJ (1997) Developmental down-regulation of receptor-mediated endocytosis of an insect lipoprotein. J Lipid Res 38: 254–265.
43. Guidugli-Lazzarini KR, do Nascimento AM, Tanaka ED, Piulachs MD, Hartfelder K, et al. (2008) Expression analysis of putative vitellogenin and lipophorin receptors in honey bee (Apis mellifera L.) queens and workers. Journal of insect physiology 54: 1138–1147.
44. Seo S-J, Cheon H-M, Sun J, Sappington TW, Raikhel AS (2003) Tissue- and stage-specific expression of two lipophorin receptor variants with seven and eight ligand-binding repeats in the adult mosquito. The Journal of biological chemistry 278: 41954–41962.
45. Soukup SF, Culi J, Gubb D (2009) Uptake of the necrotic serpin in Drosophila melanogaster via the lipophorin receptor-1. PLoS Genet 5: e1000532. doi:10.1371/journal.pgen.1000532.
46. De Gregorio E, Spellman PT, Rubin GM, Lemaitre B (2001) Genome-wide analysis of the Drosophila immune response by using oligonucleotide microarrays. Proc Natl Acad Sci USA 98: 12590–12595.
47. Ferrandon D, Imler JL, Hetru C, Hoffmann JA (2007) The Drosophila systemic immune response: sensing and signalling during bacterial and fungal infections. Nat Rev Immunol 7: 862–874.
48. Seo SJ, Cheon HM, Sun J, Sappington TW, Raikhel AS (2003) Tissue- and stage-specific expression of two lipophorin receptor variants with seven and eight ligand-binding repeats in the adult mosquito. J Biol Chem 278: 41954–41962.
49. Magrané J, Casaroli-Marano RP, Reina M, Gåfvels M, Vilaró S (1999) The role of O-linked sugars in determining the very low density lipoprotein receptor stability or release from the cell. FEBS Lett 451: 56–62.
50. May P, Bock HH, Nimpf J, Herz J (2003) Differential glycosylation regulates processing of lipoprotein receptors by gamma-secretase. The Journal of biological chemistry 278: 37386–37392.
51. Brandes C, Kahr L, Stockinger W, Hiesberger T, Schneider WJ, et al. (2001) Alternative splicing in the ligand binding domain of mouse ApoE receptor-2 produces receptor variants binding reelin but not alpha 2-macroglobulin. J Biol Chem 276: 22160–22169.
52. Sakai K, Tiebel O, Ljungberg MC, Sullivan M, Lee H-J, et al. (2009) A neuronal VLDLR variant lacking the third complement-type repeat exhibits high capacity binding of apoE containing lipoproteins. Brain Res 1276: 11–21.
53. Sepp KJ, Hong P, Lizarraga SB, Liu JS, Mejia LA, et al. (2008) Identification of neural outgrowth genes using genome-wide RNAi. PLoS Genet 4: e1000111. doi:10.1371/journal.pgen.1000111.
54. Ziegler R, Van Antwerpen R (2006) Lipid uptake by insect oocytes. Insect Biochem Mol Biol 36: 264–272.
55. Buszczak M, Lu X, Segraves WA, Chang TY, Cooley L (2002) Mutations in the midway gene disrupt a Drosophila acyl coenzyme A: diacylglycerol acyltransferase. Genetics 160: 1511–1518.
56. Thomson TC, Johnson J (2010) Inducible somatic oocyte destruction in response to rapamycin requires wild-type regulation of follicle cell epithelial polarity. Cell Death Differ 17: 1717–1727.
57. Hussain MM, Strickland DK, Bakillah A (1999) The mammalian low-density lipoprotein receptor family. Annu Rev Nutr 19: 141–172.
58. Van der Horst DJ (1990) Lipid transport function of lipoproteins in flying insects. Biochim Biophys Acta 1047: 195–211.
59. Dallinga-Thie GM, Franssen R, Mooij HL, Visser ME, Hassing HC, et al. (2010) The metabolism of triglyceride-rich lipoproteins revisited: new players, new insight. Atherosclerosis 211: 1–8.
60. Davies BS, Beigneux AP, Barnes RH, 2nd, Tu Y, Gin P, et al. (2010) GPIHBP1 Is Responsible for the Entry of Lipoprotein Lipase into Capillaries. Cell Metab 12: 42–52.
61. Beigneux AP, Davies BS, Gin P, Weinstein MM, Farber E, et al. (2007) Glycosylphosphatidylinositol-anchored high-density lipoprotein-binding protein 1 plays a critical role in the lipolytic processing of chylomicrons. Cell Metab 5: 279–291.
62. Obunike JC, Lutz EP, Li Z, Paka L, Katopodis T, et al. (2001) Transcytosis of lipoprotein lipase across cultured endothelial cells requires both heparan sulfate proteoglycans and the very low density lipoprotein receptor. The Journal of biological chemistry 276: 8934–8941.
63. Tacken PJ, Hofker MH, Havekes LM, van Dijk KW (2001) Living up to a name: the role of the VLDL receptor in lipid metabolism. Curr Opin Lipidol 12: 275–279.
64. Goudriaan JR, Espirito Santo SM, Voshol PJ, Teusink B, van Dijk KW, et al. (2004) The VLDL receptor plays a major role in chylomicron metabolism by enhancing LPL-mediated triglyceride hydrolysis. J Lipid Res 45: 1475–1481.
65. Tacken PJ, Teusink B, Jong MC, Harats D, Havekes LM, et al. (2000) LDL receptor deficiency unmasks altered VLDL triglyceride metabolism in VLDL receptor transgenic and knockout mice. J Lipid Res 41: 2055–2062.
66. Frykman PK, Brown MS, Yamamoto T, Goldstein JL, Herz J (1995) Normal plasma lipoproteins and fertility in gene-targeted mice homozygous for a disruption in the gene encoding very low density lipoprotein receptor. Proc Natl Acad Sci U S A 92: 8453–8457.
67. Parks AL, Cook KR, Belvin M, Dompe NA, Fawcett R, et al. (2004) Systematic generation of high-resolution deletion coverage of the Drosophila melanogaster genome. Nat Genet 36: 288–292.
68. Thibault ST, Singer MA, Miyazaki WY, Milash B, Dompe NA, et al. (2004) A complementary transposon tool kit for Drosophila melanogaster using P and piggyBac. Nat Genet 36: 283–287.
69. Xu T, Rubin GM (1993) Analysis of genetic mosaics in developing and adult Drosophila tissues. Development 117: 1223–1237.
70. Chou TB, Noll E, Perrimon N (1993) Autosomal P[ovoD1] dominant female-sterile insertions in Drosophila and their use in generating germ-line chimeras. Development 119: 1359–1369.
71. Bendtsen JD, Nielsen H, von Heijne G, Brunak S (2004) Improved prediction of signal peptides: SignalP 3.0. J Mol Biol 340: 783–795.
72. Strigini M, Cohen SM (2000) Wingless gradient formation in the Drosophila wing. Curr Biol 10: 293–300.

73. Yakoby N, Bristow CA, Gong D, Schafer X, Lembong J, et al. (2008) A combinatorial code for pattern formation in Drosophila oogenesis. Dev Cell 15: 725–737.
74. Stapleton M, Carlson J, Brokstein P, Yu C, Champe M, et al. (2002) A Drosophila full-length cDNA resource. Genome Biol 3: RESEARCH0080.
75. Brand AH, Perrimon N (1993) Targeted gene expression as a means of altering cell fates and generating dominant phenotypes. Development 118: 401–415.
76. Bischof J, Maeda RK, Hediger M, Karch F, Basler K (2007) An optimized transgenesis system for Drosophila using germ-line-specific phiC31 integrases. Proc Natl Acad Sci U S A 104: 3312–3317.
77. Rorth P (1998) Gal4 in the Drosophila female germline. Mech Dev 78: 113–118.
78. Queenan AM, Ghabrial A, Schupbach T (1997) Ectopic activation of torpedo/Egfr, a Drosophila receptor tyrosine kinase, dorsalizes both the eggshell and the embryo. Development 124: 3871–3880.